

---

01 Apr 1973

## Reversed and repeated lost tests of full-scale steel frames

Lauren D. Carpenter

Le-Wu Lu

Follow this and additional works at: <https://scholarsmine.mst.edu/ccfss-library>



Part of the [Structural Engineering Commons](#)

---

### Recommended Citation

Carpenter, Lauren D. and Lu, Le-Wu, "Reversed and repeated lost tests of full-scale steel frames" (1973).  
*Center for Cold-Formed Steel Structures Library*. 61.  
<https://scholarsmine.mst.edu/ccfss-library/61>

This Technical Report is brought to you for free and open access by Scholars' Mine. It has been accepted for inclusion in Center for Cold-Formed Steel Structures Library by an authorized administrator of Scholars' Mine. This work is protected by U. S. Copyright Law. Unauthorized use including reproduction for redistribution requires the permission of the copyright holder. For more information, please contact [scholarsmine@mst.edu](mailto:scholarsmine@mst.edu).

BULLETIN NO. 24, APRIL, 1973—L. D. Carpenter and L. W. Lu—REVERSED AND REPEATED LOAD TESTS OF FULL-SCALE STEEL FRAMES

# STEEL RESEARCH for construction

## REVERSED AND REPEATED LOAD TESTS OF FULL-SCALE STEEL FRAMES

*by Lauren D. Carpenter and Le-Wu Lu*

Committee of Structural Steel Producers

Committee of Steel Plate Producers

**american iron and steel institute**

150 East 42nd Street, New York, N.Y. 10017



#30  
CONSTRUCTION

BULLETIN NO. 24, APRIL, 1973

# Reversed and Repeated Load Tests of Full-Scale Steel Frames

Lauren D. Carpenter and Le-Wu Lu

*Fritz Engineering Laboratory  
Department of Civil Engineering  
Lehigh University  
Bethlehem, Pennsylvania*

Committee of Structural Steel Producers

•

Committee of Structural Plate Producers

**american iron and steel institute**

150 East 42nd Street, New York, N.Y. 10017

## ACKNOWLEDGMENTS

The work reported herein was performed at Fritz Engineering Laboratory, Department of Civil Engineering, Lehigh University. Dr. David A. VanHorn is the Chairman of the Civil Engineering Department and Dr. Lynn S. Beedle is Director of Fritz Engineering Laboratory. The results presented form part of an investigation on "Behavior of Steel Frames Subjected to Repeated Loading," sponsored by the American Iron and Steel Institute. Technical guidance is provided by a special Task Force organized by the Institute whose membership includes: I. M. Viest (Chairman), G. C. Berg, H. J. Degenkolb, G. C. Driscoll, Jr., T. V. Galambos, W. C. Hansell, C. W. Pinkham, E. P. Popov and J. L. Stratta. The authors gratefully acknowledge the support given by the Institute and the advice received from the members of the Task Force.

Appreciation is also extended to the authors' many associates at Fritz Laboratory for their day and night assistance during the many phases of the experiments. Particular long term assistance was provided by Messrs. Basil Kattula, Richard A. Schmidt, Robert J. Kirchberger and Shosuke Morino. The assistance of Mr. Kenneth R. Harpel, Laboratory Superintendent, and his technicians in the preparation for and carrying out of the experiments is gratefully acknowledged. The report was typed by Miss Karen Philbin and the tracing of figures was done by Mr. John Gera and Mrs. Sharon Balogh.

## CONTENTS

Acknowledgments .....	i
Abstract .....	iv
1. Introduction .....	1
1.1 Dynamic vs. Static Response .....	1
1.2 Previous Research .....	1
1.2.1 Experimental Behavior of Simple Specimens .....	1
1.2.2 Experimental Behavior of Members and Frames .....	1
1.3 Scope of Investigation .....	2
2. Design of Test Frames .....	4
2.1 Design Parameters .....	4
2.2 Analysis and Design of Frames A and B .....	4
2.3 Frame C Design .....	5
2.4 Frame D Design .....	6
2.5 Frame E Design .....	7
3. Testing Technique .....	7
3.1 Introduction .....	7
3.2 Testing Technique .....	8
3.2.1 Basic Testing Schedule .....	8
3.2.2 General Testing Arrangement .....	8
3.3 Material and Cross-Sectional Property Measurements .....	9
3.4 Mechanical and Electrical Measurements .....	10
4. Experimental Behavior of Test Frames .....	10
4.1 Introduction .....	10
4.2 Single-Story Frame A .....	10
4.3 Three-Story Frame B .....	11
4.4 Single-Story Frame C with Noncompact Beam .....	13
4.5 Single-Story Frame D with Minor Axis Column Orientation .....	15
4.6 Two-Story Frame E with Hinges in Columns and Beams .....	17
5. Observations Based on Experimental Results .....	19
5.1 Comparison of Maximum Experimental Loads with Predicted Loads for Monotonic Loading Condition .....	19
5.2 Stability of Hysteresis Loops .....	20
5.3 Shape of Hysteresis Loops .....	20
5.4 Connection Details .....	21
5.5 Behavior of Frames with Noncompact Beams .....	21
5.6 Behavior of Frames with Columns Oriented for Minor Axis Bending .....	21
5.7 Behavior of Frames with Plastic Hinges in Columns and Beams .....	21
6. Summary and Conclusions .....	22
7. References .....	23
8. Appendixes .....	24
Appendix 1 Aseismic Forces of the Eight-Story Prototype Frame .....	24
Appendix 2 Design Checks for Test Frames .....	25
Appendix 3 Cross-Sectional and Mechanical Properties .....	31
Appendix 4 Locations for Strain Gages, Rotation Gages and Deflection Measurements .....	32

## ABSTRACT

Two series of tests are described to investigate the behavior of five full-sized single-bay A-36 steel frames subjected to constant gravity loads on the beams and columns and cycles of reversed and repeated lateral displacements. The tests represent parts of an eight-story ductile steel frame subjected to simulated earthquake loading.

The first test series involved a single-story and a three-story frame. The frames were designed and detailed to reflect current aseismic design practice. The inelastic behavior was confined to the beams and the panel zones were stiffened according to AISC specification requirements.

The second test series expanded into three particular problems. The effect of local buckling of the beams was evaluated in a single-story frame. Another single-story frame with columns oriented for minor axis bending was tested to study the behavior of the columns in the inelastic range and of the beam-to-column connections. A two-story frame was tested to study the behavior with the plastic hinges in the columns as well as the beams.

The test results demonstrated the considerable load-carrying capacity and ductility of steel frames when subjected to the reverse lateral displacement program. The experimental maximum lateral loads exceeded by from 17 to 40% the analytical maximum loads predicted for monotonic static loading. The stability of the lateral load vs. deflection hysteresis loops is shown at lateral deflection amplitudes up to 14 times the working load lateral displacement. This corresponds to a drift index of 0.043.

The role of strain hardening, local flange buckling in columns and noncompact beams, inelastic column moments and the effect of the gravity loads are described.

The beam-to-column connection and panel zone stiffening details are evaluated. Maximum moments applied to the connections exceeded the plastic moment of the beams by about 10 to 20%. The connections transmitted these increased and repeatedly applied moments in spite of the fact that plastic beam moments were used to design the connections. Stable hysteresis behavior was obtained with panel zone shear stiffening and welds between the beam web and column flange omitted during several maximum amplitude cycles at the end of one frame test.

# Reversed and Repeated Load Tests of Full-Scale Steel Frames

LAUREN D. CARPENTER

LE-WU LU

## 1. Introduction

The design of buildings in areas of high seismic activity is based on past experience of concerned designers. The current code provisions (1)<sup>1</sup> assume inelastic behavior of the building's structural frame and nonstructural components. The large amount of masonry used in older structures permitted considerable dissipation of the energy imparted to the building by an earthquake. In newer steel framed construction with curtain walls, a significant proportion of the energy dissipation is due to the inelastic behavior of the steel framing. It is therefore necessary for the designers of the modern framed structures to be able to estimate the inelastic strength and the energy dissipation capacity of the buildings.

### 1.1 Dynamic vs. Static Response

Dynamic analyses of multistory steel buildings are performed to evaluate the behavior of buildings during earthquakes.

Preliminary experimental load vs. deflection hysteresis loops obtained from static and dynamic tests on simple specimens show that the hysteresis loops have nearly duplicate shapes (3, 4). In addition, since the effects of strain rate in structural steel are considered to be small during earthquake loadings (5), a small increase in yield stress of the steel could be used to account for the dynamic effects (6). Therefore, the static load versus deformation characteristics of the structural elements and of the structure subjected to combined lateral and gravity loads are the basic information necessary to perform the dynamic analyses.

<sup>1</sup> The numbers in parentheses refer to the list of references at the end of this bulletin.

## 1.2 Previous Research

The following articles review some of the previous experimental research on simple specimens, members and frames subjected to various reversed loading conditions.

**1.2.1 Experimental Behavior of Simple Specimens** The cyclic stress vs. strain behavior of small axially loaded pieces of steel has been investigated for the usual purpose of studying the fatigue characteristics of the material rather than the basic load-carrying properties of the materials. Benham and Ford (7) and Tavernelli and Coffin (8), for example, were concerned primarily with relating the nominal stress vs. plastic strain results to fatigue behavior. Although fatigue behavior is recognized as a possible governing factor in the overall behavior of a complete frame, emphasis should be placed on the load vs. deformation behavior of the frames subjected to alternating loads. These alternating loadings in no way imply an equal amplitude strain or stress cycling throughout each "fiber" of each cross section of the members of the frame.

**1.2.2 Experimental Behavior of Members and Frames** A considerable number of tests have been performed on structural components and simple structures subjected to repeated and reversed loads (9). In one series of tests, cantilever beams were tested to study the basic behavior of these beams subjected to reversed loads (10). Further studies in the series included welded and bolted beam-to-column connections typical of those used in earthquake resistant design (11–15). These cantilever beam tests showed a remarkable stability of the hysteresis loops for very high strain amplitudes. Significant local buckling did not signal immediate loss of capacity for these beams which

had “compact” flanges and relatively close bracing spacing. Low cycle fatigue and attention to welding details were indicated as necessary design parameters since most of the tests were terminated by fractures. Other recent cantilever beam tests have indicated that proper lateral support is required to insure stable hysteretic behavior of a cantilever (16). Since both the moment vs. curvature and the load vs. deflection hysteresis loops have remarkably stable shapes, the cantilever beam test results imply that a practically constant amount of energy absorption can be depended upon per cycle at each level of strain (17–19). The test results also show that the areas enclosed by the hysteresis loops increased with increasing displacement magnitude (12). Similar behavior has been exhibited during reversed bending tests of different types of beams (20–22).

Beam-columns bent in double and single curvature have been tested under constant axial loads and alternating end moments (23, 24). More comprehensive experiments including interaction of beams subjected to repeated and reversed loading with axially loaded columns have been reported (27–30). The results of these tests showed that for columns with small and nearly constant axial loads stable hysteresis behavior is usually generated.

As an adjunct to tests of multistory frames designed to study the static behavior of the frames subjected to monotonic lateral load applications, these full-scale frames were subjected to reversed loading after very large inelastic deformations had occurred due to the initial loading (31–33). These tests were all terminated after one or two cycles and gave an indication of the possible lateral load-carrying capacity of the full-scale frames subjected to reversed loading.

More comprehensive experimental programs directly relating to the reversed load problem were reported by Sidebottom and Chang (34) and Tanabashi et al. (35). The former authors reported tests on tension-compression and compression-tension tests of axially loaded specimens as well as reversed bending tests of simple beams. The latter authors reported on an extensive testing program on axially loaded specimens at various load amplitudes and also subjected simple beams of wide-flange cross section to reversed loadings. Apparently only in these two investigations have attempts been made to predict member behavior based on the experimental behavior of simple specimens subjected to similar loadings.

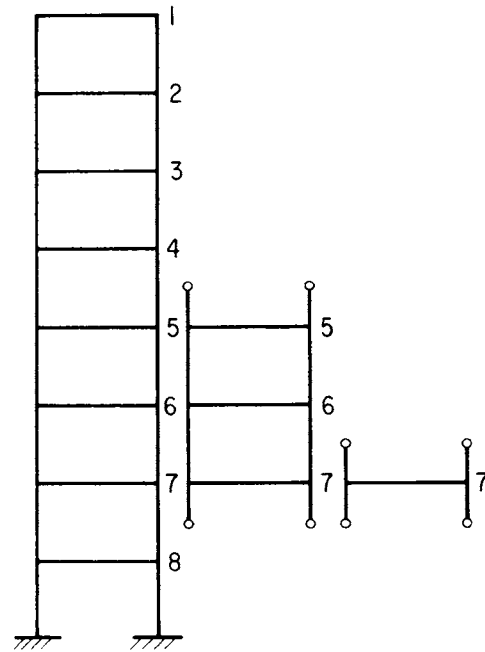


FIGURE 2.1. Prototype structure and test frames

In the experiments by Popov (11–15), Kurobane (36), Chipman (37) and Sherborne et al. (20, 21) with approximately equal amplitude strain cycling, attempts were made to correlate applied loadings and corresponding strains. Arnold, Adams and Lu (32), and AlMuti (4) compared their experimental results with predictions based on a simplified monotonic stress vs. strain curve.

The essential observation to be made from inspection of these tests is that a similar type of hysteresis loop is generated for a rolled steel member in bending as for a short specimen subjected alternately to tensile and compressive loading or straining.

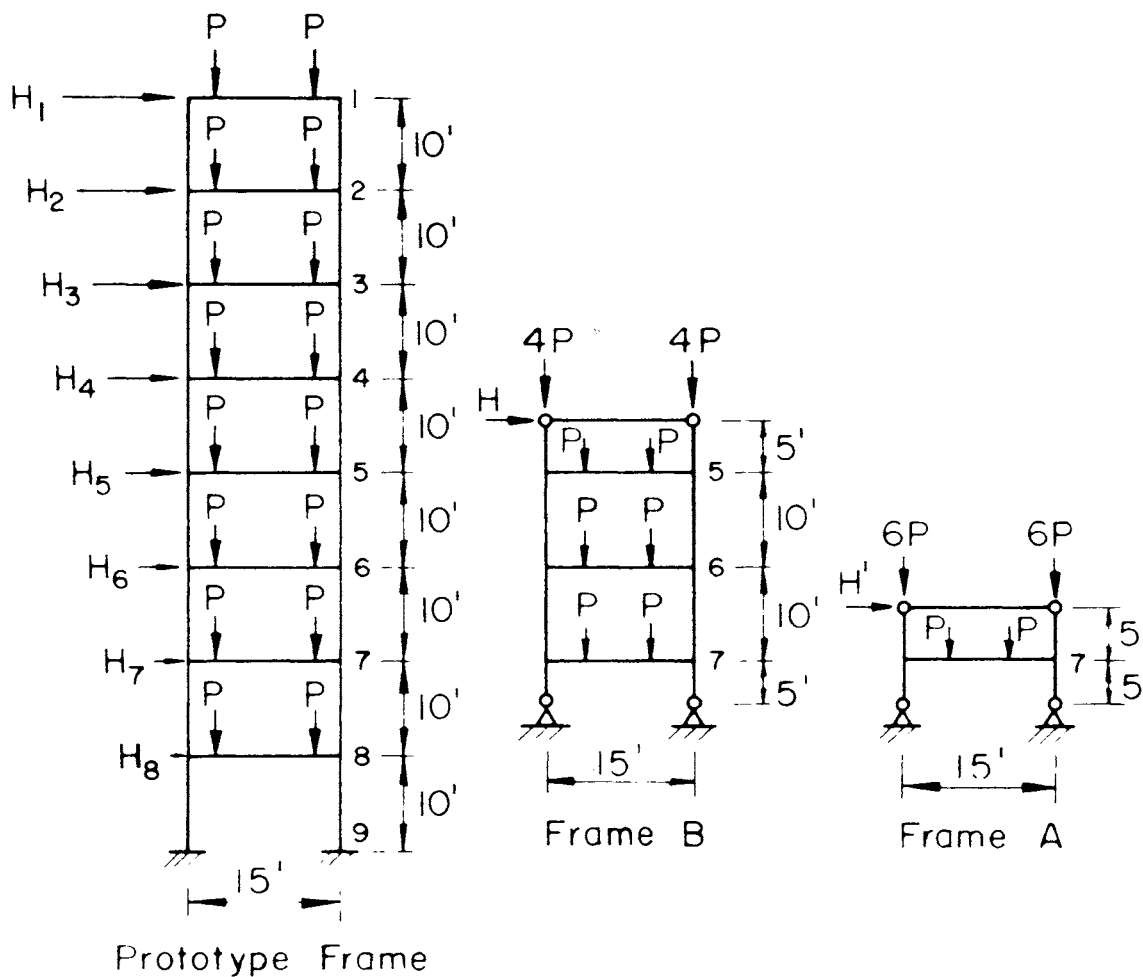
### 1.3 Scope of the Investigation

Two series of tests were performed on single-bay steel frames and evaluated with respect to the behavior of the frames subjected to constant gravity loads and a program of cyclically applied lateral displacements. The emphasis of the testing program is on the behavior of low multistory steel frames of A36 steel subjected to simulated earthquake conditions.

The first test series involved a single-story and a three-story frame. The frames were designed and detailed to reflect current aseismic design practice. The inelastic behavior was confined to the beams and the panel zones were stiffened according to AISC Specification requirements.

The second test series expanded into three particular problems. The effect of local buckling of the beam was evaluated in a single-story frame.





Working Loads Used in the Design of Test Frames

Gravity

Dead Load	80psf = 1440 lbs/ft	} 18 ft Bent Spacing
Full Design Live Load	80psf = 1440 lbs/ft	

$$P_{DL} = \frac{W_{DL} (L)}{2} = \frac{1440 (15)}{2} = 10.8^k$$

$$P_{LL} = 10.8^k ; P_{LL} (design) = 60\% P_{LL} = 6.48^k$$

$$P_{TOTAL} (design) = 17.28^k$$

Earthquake

$$H = H_1 + H_2 + H_3 + H_4 + H_5 = 5.19^k$$

FIGURE 2.2 Design loading of the test frames

Another single-story frame with columns orientated for minor axis bending was tested to study the behavior of the columns in the inelastic range and of the beam-to-beam column connections. A two-story frame was tested to study its be-

havior with the plastic hinges in the columns as well as the beams.

The following chapters describe the design of the steel frames subjected to aseismic code lateral forces, the technique developed to test these

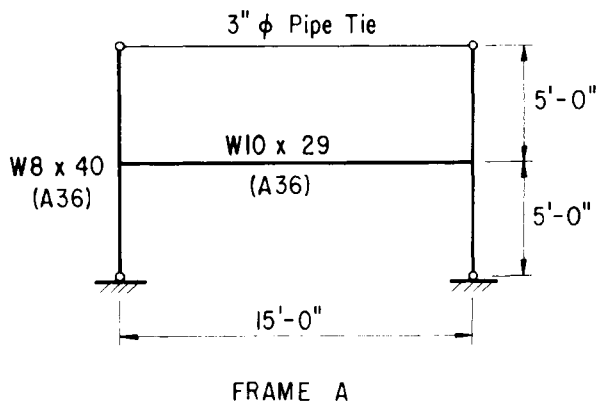


FIGURE 2.3a. Geometry and member sizes of Frame A

frames, and the experimental behavior of these frames. Observations based on the experimental results are described in later chapters.

## 2. Design of Test Frames

### 2.1 Design Parameters

The test frames were designed by following the aseismic design practice. The lateral forces are based on the current aseismic design code for the eight-story, single-bay prototype structure shown in Figure 2.1. The columns of the prototype frame are likely to be bent in double curvature and have points of inflection near their mid-heights when lateral loads are applied. Therefore, assemblages can be formed by subdividing the prototype frame at the mid-heights of the columns. A three-story assemblage that would represent levels 5, 6 and 7 of the prototype frame is shown in Fig-

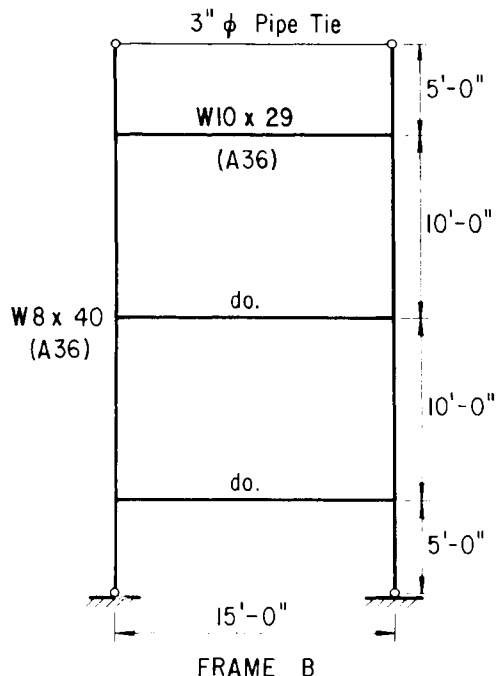


FIGURE 2.3b. Geometry and member sizes of Frame B.

ure 2.1. A single-story frame, Frame A, was then selected as the lowest story of the three-story frame, Frame B, and loaded accordingly. Frames C and D were subjected to the same conditions as Frame A. Frame E is a similarly loaded two-story assemblage.

Eighty pounds per square foot were selected for full dead loads and also for full live loads with an average live load reduction of 40% applied to both beams and columns. The gravity loads applied to the frames were based on an 18-ft spacing of each frame in the prototype building. The total tributary floor loading was placed as two equal concentrated loads at approximately the quarter points of the beam span.

Since the portion of the building selected for design, analysis and testing is in a region of small variation in the total aseismic design shear, the working design shear was selected as the summation of the aseismic shears through level 5 for Frame B as shown in Figure 2.2. The determination of the aseismic design shears for the various floor levels is illustrated in Appendix 1. The working shear is equal to approximately 3½% of the sum of the dead loads through level 7 and causes a static drift of (story height)/350 per story. The geometry of the frame and the member sizes were selected to have ratios of column-to-beam stiffnesses which are representative of buildings designed for seismic areas. The beam-to-column connection details were also similar to the fully welded connections used in Popov's cantilever beam tests (11-15). However, shear stiffening was also provided in the panel zones of the frames.

### 2.2 Analysis and Design of Frames A and B

An approximate design and subsequent analysis were performed for Frame B subjected to gravity and combined gravity and lateral loads to find the preliminary member sizes. The preliminary frame was then analyzed to determine the bending moment and axial force distribution. The analysis was carried out on the frame under working gravity load alone and then the working value of the horizontal load was added. The results obtained permitted comparing the adequacy of the beams and columns with the allowable stresses specified in the AISC (American Institute of Steel Construction) Specification. The comparisons are given in Appendix 2. The final member sizes selected for Frame B are shown in Figure 2.3b. The same member sizes were also adopted for Frame A (Fig. 2.3a).

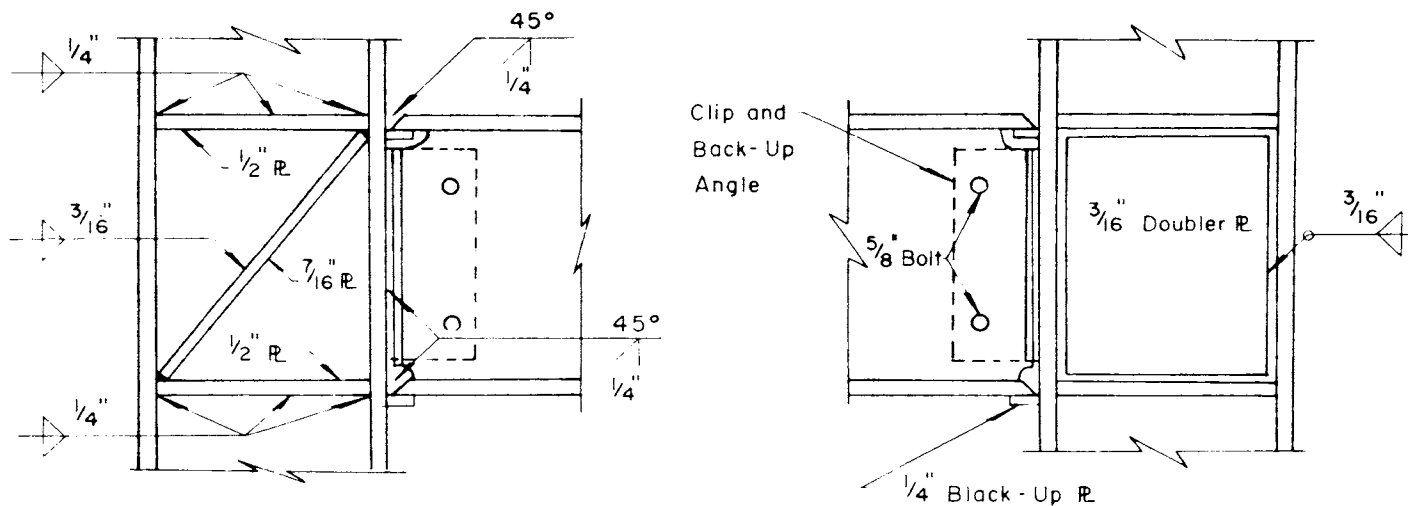


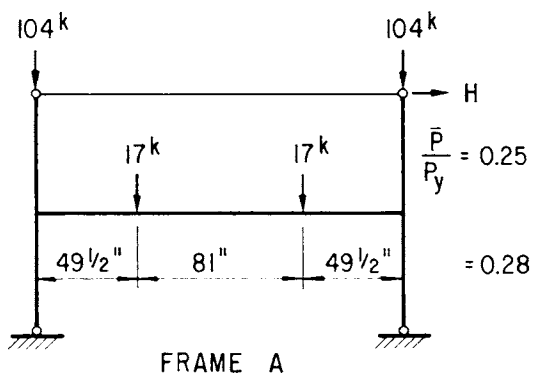
FIGURE 2.4. Beam-to-column connections of Frames A and B

The horizontal and shear stiffening of the panel zone at the beam-to-column connections were selected by plastic design requirements (39). The details of the connections are shown in Figure 2.4.

To find the complete load vs. deflection curve, each frame was subjected to a monotonically increasing horizontal force with the constant gravity loads at the working value as shown in Figures 2.5a and 2.5b for Frames A and B. A second-order elastic-plastic analysis that included the  $P-\Delta$  moment in each story was carried out for these frames. The load vs. deflection curve for Frame A, Figure 2.6, indicates that the frame instability load and the plastic mechanism load coincide at a lateral load of 14.8 kips. However, the curve in Figure 2.7 shows Frame B to be unstable at a load of 15.3 kips before a mechanism is formed.

### 2.3 Frame C Design

The purpose of this test is to evaluate with respect to Frame A the behavior of a frame which has local buckling occurring in the beam flanges



$\bar{P}$  = Axial Load in Column,  $P_y$  = Axial Yield Load of Column

FIGURE 2.5a. Loads and axial thrust ratios of Frame A

similar to that experienced in Popov's tests (11-15). Therefore the test frame was selected to be a duplicate of Frame A except with a beam with a high flange width-to-thickness ratio. The W10×29 used in Frame A had a  $b/t$  ratio of 11.5. The beam used in Frame C was welded from three plates to have nearly the same section modulus and fully plastic moment as the W10×29. The final cross-section selected has a  $b/t$  ratio of 21 as shown in Figure 2.8. The inelastic behavior of Frame C would be expected to be approximately the same as Frame A if local buckling of the beam flanges does not have an effect on the lateral load capacity of the frame.

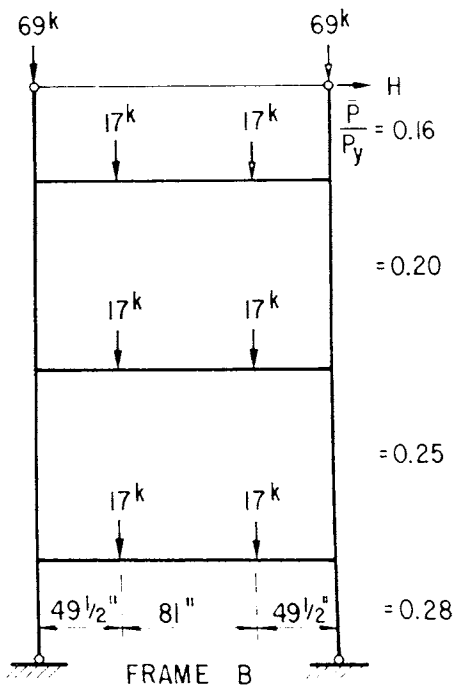


FIGURE 2.5b. Loads and axial thrust ratios of Frame B

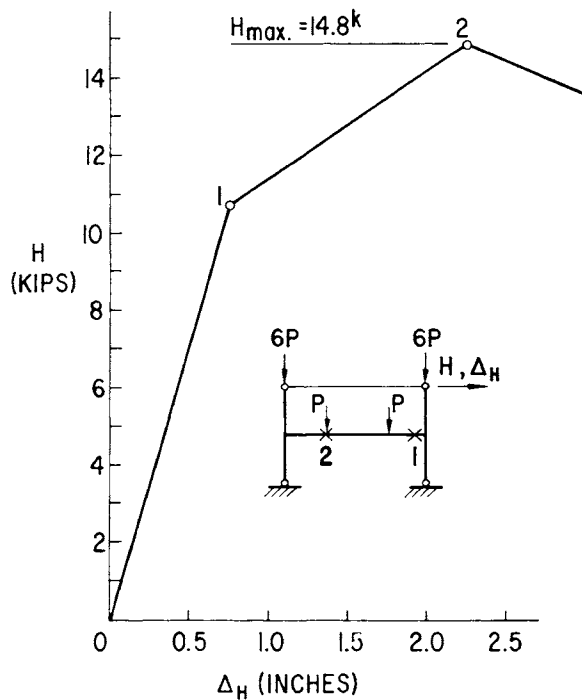


FIGURE 2.6. Load-deflection curve for Frame A

#### 2.4 Frame D Design

The main emphasis in the test of Frame D was the minor axis orientation of the columns, and the corresponding minor axis beam-to-column connection. The behavior of partially inelastic columns under cyclic bending is also investigated. The beam and column sections shown in Figure 2.9 were selected to satisfy the above criteria as well as keeping the elastic stiffness of the frame and its

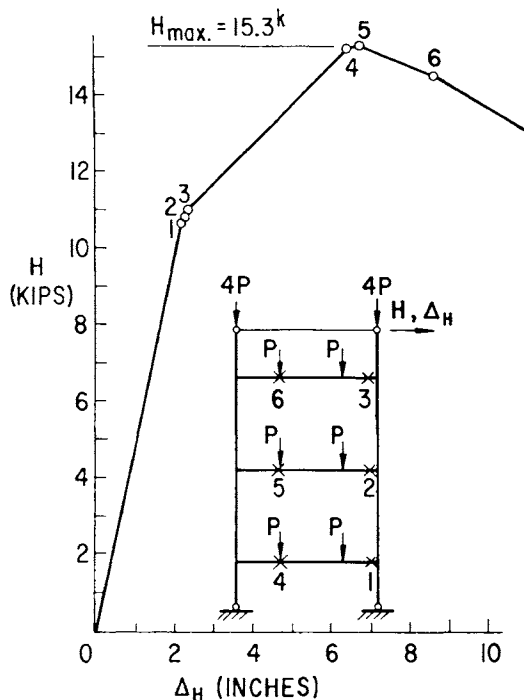


FIGURE 2.7. Load-deflection curve for Frame B

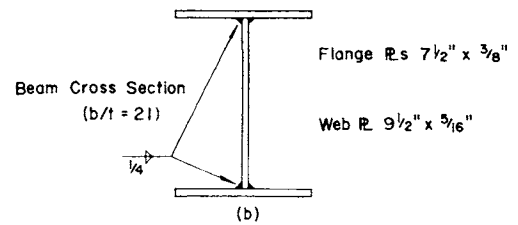
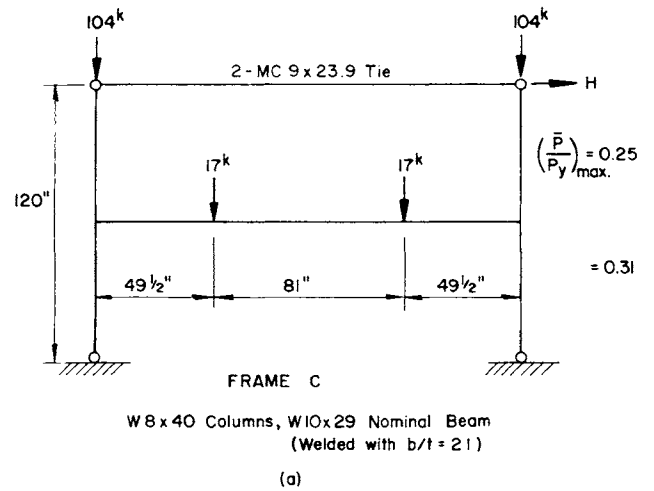


FIGURE 2.8. Frame C and beam cross section

maximum monotonic load capacity similar to Frame A. The comparisons with AISC requirements are given in Appendix 2.

The load vs. deflection curve for Frame D is shown in Figure 2.10. The maximum lateral load is 17.1 kips at the formation of a beam mechanism

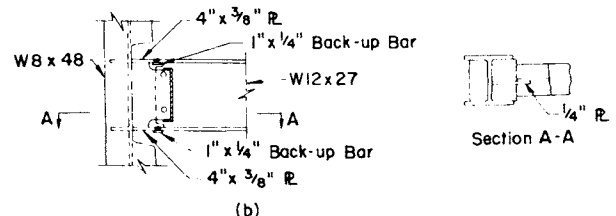
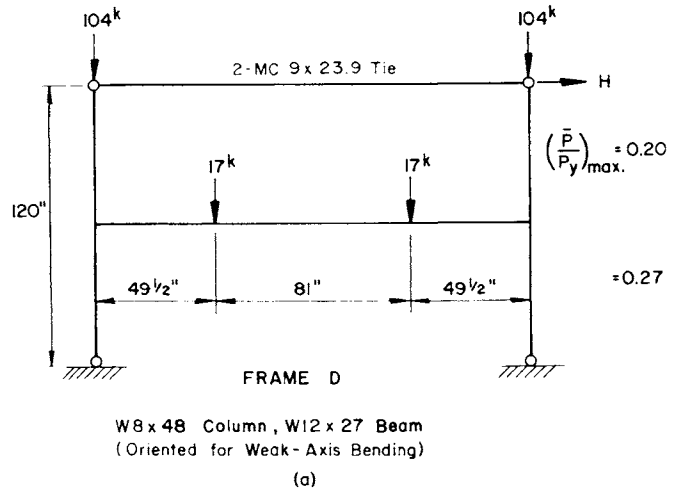


FIGURE 2.9. Frame D and connection details

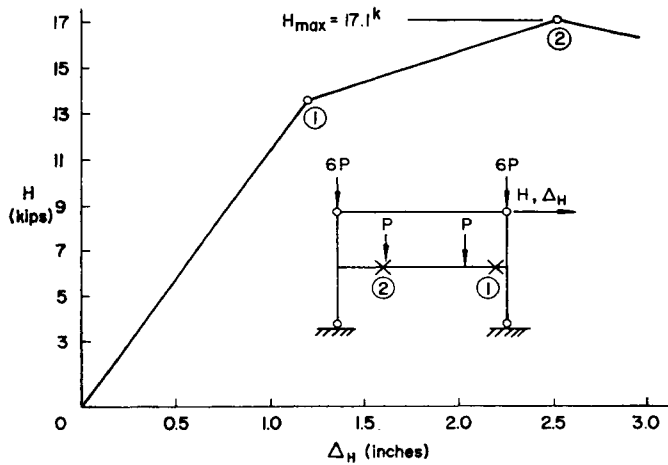


FIGURE 2.10. Load-deflection curve for Frame D

similar to Frame A or C. What is not clearly apparent in this elastic-perfectly plastic analysis is that the moments in the column are greater than yield but less than the fully plastic moment capacity reduced for axial load effect. The moment exceeds the yield moment by about 1.2 but is less than the fully plastic moment which is about 1.5 times the yield moment.

### 2.5 Frame E Design

The purpose of the test of two-story Frame E was to evaluate the behavior of a frame with

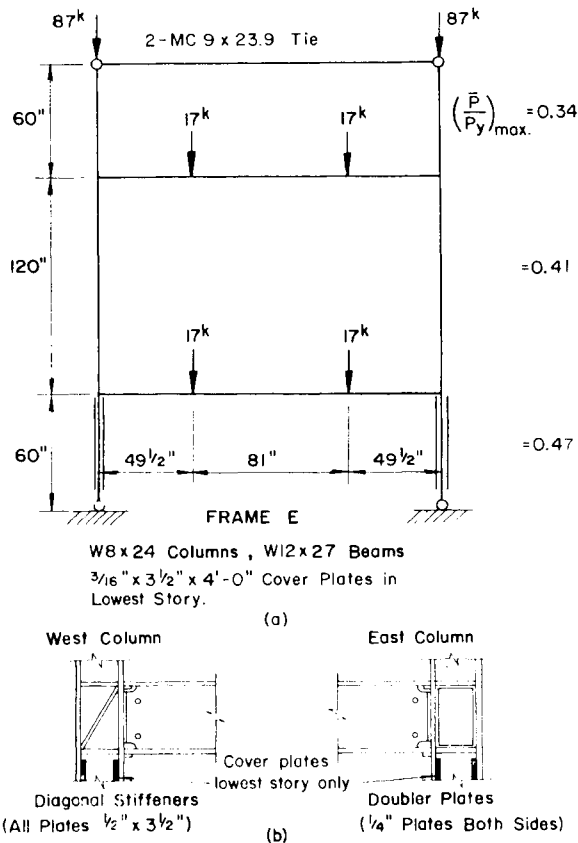


FIGURE 2.11. Frame E and connection details

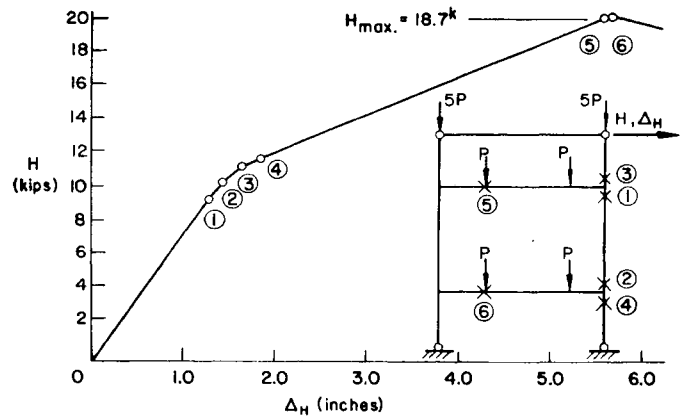


FIGURE 2.12. Load-deflection curve for Frame E

plastic hinges in the columns (orientated for major axis bending) and in the beams. The frame stiffness and strength were also similar to those of Frame A. The member sizes of this frame are shown in Figure 2.11. The comparisons with AISC Specification requirements are given in Appendix 2. The W8×24 section selected for the columns was slightly under-sized. This was necessary in order to insure that plastic hinges would form first in the columns.

The load vs. deflection curve for Frame E is shown in Figure 2.12. The maximum load of 18.7 kips and the sequence of plastic hinge formation are also shown. The general failure characteristics are similar to the other frames except that the hinge at the end of the beam has been displaced into the column above and below the beam-to-column intersection. To avoid a panel mechanism in the lowest story of the assemblage, the columns in that story were reinforced by cover plates.

## 3. Testing Technique

### 3.1 Introduction

The frames were tested by subjecting them to constant gravity loads at the working value and a program of statically applied cyclic lateral displacements of the top of the frames. The lateral displacement programs were similar to those used by Popov on cantilevered beams (11-15, 17-19).

Initially the gravity loads were applied to the frames and then sets of lateral displacements of increasing amplitudes were applied to the frames in a cyclic manner. The lateral displacements were cycled equally about the vertical position of the frame in a step wise fashion from small to large amplitudes. In each case the amplitudes to be cycled were selected to bracket the plastic hinge occurrences as determined by the elastic-plastic

analysis and other intermediate points on the respective load-deflection curves. For displacements in the elastic range the frames were subjected to three cycles at each amplitude and for inelastic range displacements five cycles were imposed. The number of repetitions of each cycle amplitude was set to observe the stability of the hysteresis loops at the various amplitudes of deflection and inelastic conditions of the frames. The amplitudes selected for the test frames are described in detail in Chapter 4.

### 3.2 Testing Technique

**3.2.1 Basic Testing Schedule** Each frame was commercially bid on and fabricated by structural fabricators from working drawings. The shop fabricated members were erected in the basic testing arrangement and aligned by transits to be vertical in two directions. The beams were leveled and aligned. The frame was instrumented and initial readings were taken. The beam-to-column connections were then field welded in the laboratory by the structural fabricator. The gravity loads were then added incrementally to the columns to verify and adjust the column stresses to "alignment under load" conditions. The gravity loads were increased to the dead load portion of the total load on all members.

At this point in the test several cycles at different amplitudes of lateral displacement were applied for the purpose of making a complete checkout of the measuring devices and the experimental data generated. These amplitudes were selected such that the frame remained essentially elastic.

After completely unloading the frame, the main portion of the testing program was started by applying the full gravity loads to the columns and to the beams incrementally. At this point sets of cycles of increasing lateral displacement amplitudes were applied to the top of the frame until the test was nearly completed. At the end of each test the frame was displaced in one direction to the maximum amount possible for the displacement apparatus used in the test.

**3.2.2 General Testing Arrangement** Various pieces of hardware were procured or fabricated and then assembled into the general arrangement for testing the frames in the manner previously described. Figure 3.1 is an overall view of the test setup for Frame B. Gravity loads were applied to each beam by utilizing gravity load simulators. Each simulator was attached to a load spreader beam which in turn applied load to two points on the beam through load cells and load

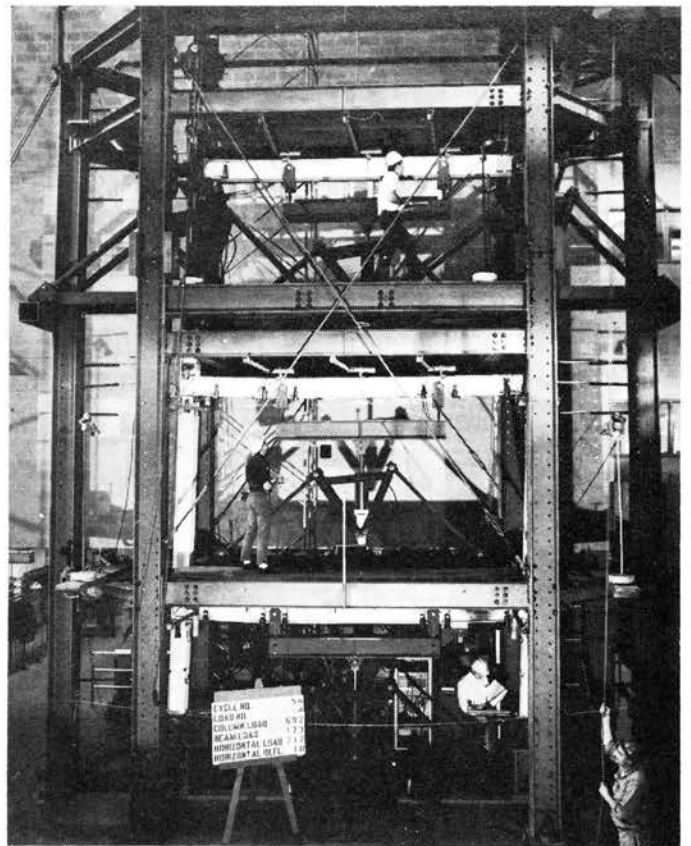


FIGURE 3.1. Testing arrangement for Frame B

hangers. Each load hanger was attached to a shaft passing through the beam at its mid-depth. The gravity load in each column was applied by two simulators. One simulator on each side of the column was attached through a load cell and a load hanger to the ends of a large diameter shaft passing through the top of the column.

A common pressure source was used for the beam simulator jacks and another independent common source was used for the simulators applying loads to the columns. Each air-to-oil pump source was self regulating to hold the gravity loads essentially constant throughout the test.

The boundary conditions imposed on the frames required zero moments at the assumed points of inflection above and below the main portions of each frame as described in Chapter 2. Therefore, the base of each column was bolted to a specially designed hinged end fixture which utilized a larger diameter shaft passing through roller bearings in adjacent pillow blocks. To distribute the applied lateral force, a link member was connected between the shafts passing through the top half story columns. Each end of the link member was attached to the shafts by means of roller bearing assemblies.

The lateral displacement of the top of the frame was accomplished by either turnbuckles on each

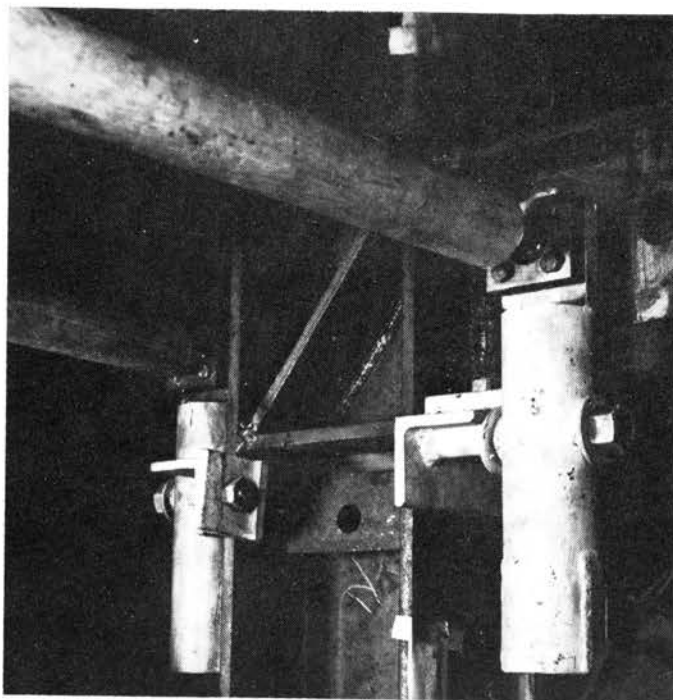
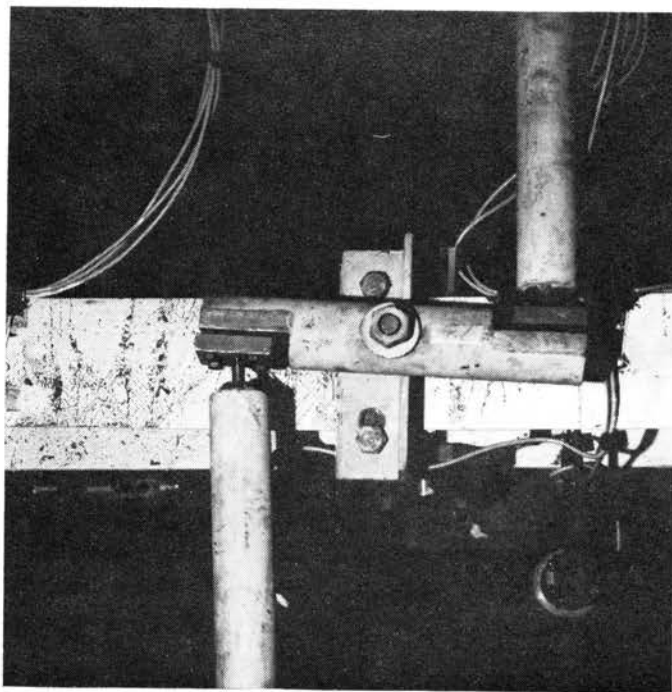


FIGURE 3.2. Attachment of lateral bracing to beam and column

side of the top of the frame pulling alternately or by a mechanical jack attached to the center of the link member. For either case, load cells were connected in series with the displacement apparatus to measure the corresponding lateral forces.

Special bracing linkages were used to brace the frame without offering any restraint to in-plane

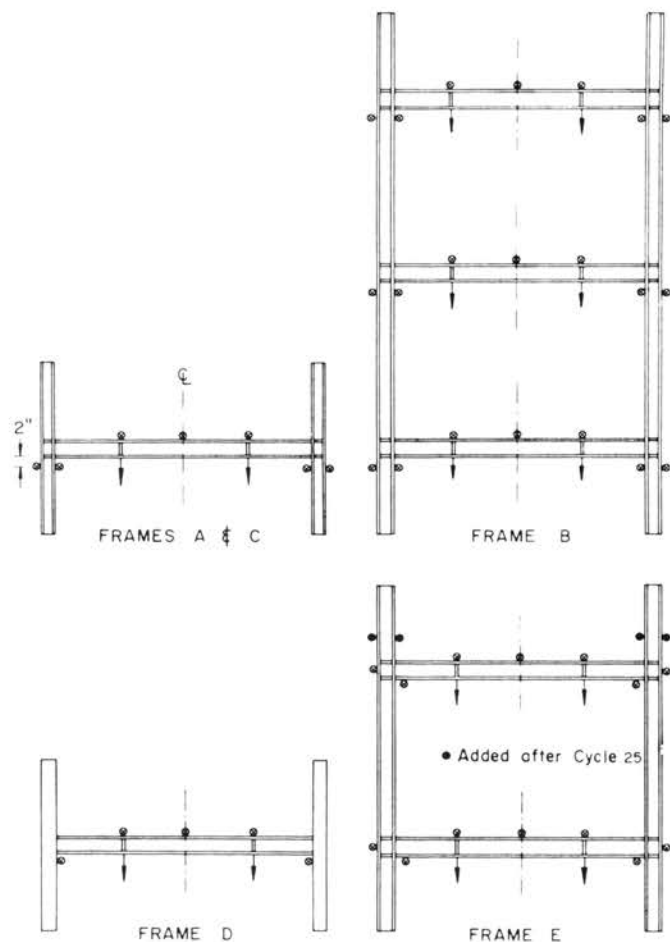


FIGURE 3.3. Locations of lateral braces

movements (Fig. 3.2). The top flange of each beam was supported laterally at each load point and at center span. In a building, the floor system would provide lateral support for the top flange. In addition, the lower flange was effectively braced laterally by attaching the brace to the inside of the adjoining columns two inches below the beam flange. Braces were also added on the outside of each column opposite the interior braces. These column braces approximate lateral support from beams framing to the column web. The location of the beam end column braces are shown in Figure 3.3 for all the frames tested.

### 3.3 Material and Cross-Sectional Property Measurements

Preliminary data in each test consisted of testing three small specimens cut from each end of every member as well as the stiffener material. These specimens were tested in monotonic tension at a very slow rate to observe the elastic, plastic and strain hardening characteristics of the as-delivered material. A summary of the measured yield stresses of all the material used to fabricate the test frames is given in Appendix 3.

The actual dimensions of each end of each member were measured and the cross-sectional area and section modulus were computed. In addition, from the actual dimension and the static yield levels measured in the tension tests the plastic moment values and axial yield loads of the members were computed. This information is also summarized in Appendix 3.

### 3.4 Mechanical and Electrical Measurements

Various types of data were taken during the tests. Vertical loads were measured through the applied jack pressure and by means of load cells at the points where the jack loads were applied to the frame. Horizontal loads were measured by load cells which were in series with the lateral displacement apparatus. Lateral deflections of several points on each column were measured by linear potentiometers or transits or a combination of both. Vertical deflections along the beams were measured by surveyor's levels. Rotations at various points throughout the frame were measured mechanically, electrically or by both methods. Strains throughout the frame were measured by means of electrical resistance strain gages. The electrical measurements were digitized and automatically punched onto computer cards, whereas various mechanical measurements were recorded by hand and then punched onto the cards. In addition, the progression of yielding and other pertinent data were logged throughout the tests by hand or photographically.

The locations of strain gages, rotation gages and the various points around the test frames where the vertical or horizontal deflections were measured are given in Appendix 4.

## 4. Experimental Behavior of Test Frames

### 4.1 Introduction

The following articles describe the basic test results from the five frame tests. The descriptions will be concerned primarily with:

1. The shapes of the lateral load vs. deflection hysteresis curves.
2. The magnitudes of the lateral load attained during the test.
3. The stability of the size and shape of the load vs. deflection hysteresis curves during repeated cycling at each constant deflection amplitude.
4. The local behavior of the members and their component plates as well as connections and fabrication details.

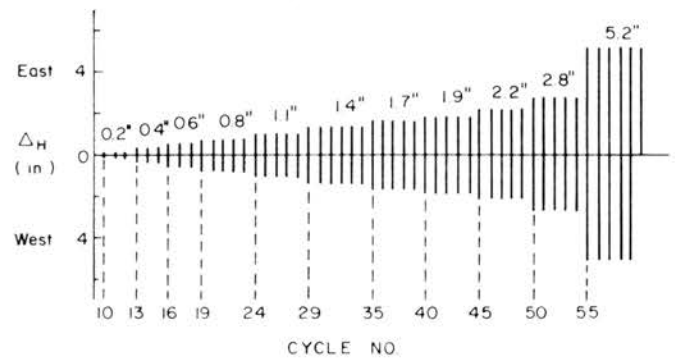


FIGURE 4.1. Displacement program for Frame A

### 4.2 Single-Story Frame A

Fifty-one cycles at various amplitudes of lateral displacements were applied to Frame A with a maximum displacement amplitude of 5.2 in. The largest cycled displacement was about 14 times the deflection at the working value of lateral load.

Initially, after alignment of the axial loads in the columns had been completed, the preliminary phase of the test began. The dead load portion of the total gravity loads was applied to the beam and columns. Then, several cycles of elastic range displacements were applied to verify the complete testing arrangement.

The basic gravity loads applied to the test frame during the main portion of the test were 17.3 kips at each load point (at 0.275 L from the center of each column) and a total of 103.8 kips applied to the top of each column.

The controlled lateral displacements were then applied to the top of the frame. The particular lateral displacement program adopted for this frame consisted of three cycles at amplitudes of 0.2, 0.4 and 0.6 in. Then five cycles were applied at amplitudes of 0.8, 1.1, 1.4 (6 cycles), 1.7, 1.9, 2.2, 2.8 and 5.2 in. and the test stopped. Figure 4.1 gives the entire displacement program and the numbers assigned to the various cycles.

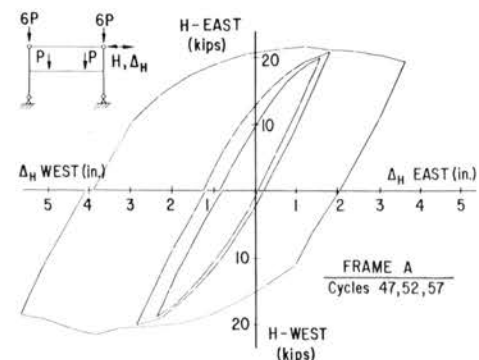


FIGURE 4.2. Load vs. deflection curves at selected displacement amplitudes for Frame A



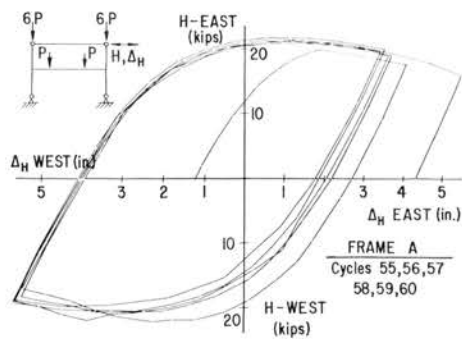


FIGURE 4.3. Stability of load vs. deflection curves for Frame A

The hysteresis loops for selected displacement amplitudes for Frame A are shown in Figure 4.2. The maximum load obtained is about 40% greater than the maximum load indicated in Chapter 2.

As in the case of the hysteresis loops generated for the cantilever beam tests, the repetitions of the cycles at all amplitudes indicated stable hysteresis loops. However, for the frame the downward sloping portion of the curves between the deflection at the maximum load to the maximum deflection shown in Figure 4.3 is important. After the maximum load was reached, the frame usually would become unstable because of the  $P-\Delta$  effect. Figure 4.3, however, indicates hysteresis loops are always stable and highly reproducible.

The test shows the significant influence of strain-hardening. On each of the large amplitude cycles of the frame, once the deflection at the maximum lateral load has been exceeded, the lateral load-carrying capacity dropped off much more slowly when compared with the theoretical monotonic predictions that ignored strain hardening.

The curved shape of the hysteresis loops for frames subjected to reversed loading is caused not only by the Bauschinger effect in the material but also by the reduction in frame stiffness due to the spread of yielding at the plastic hinge locations as indicated in Figure 4.4. The general shape of the loops is also affected by the yielding of the beam-to-column connections (Fig. 4.5).

Figure 4.6 shows the moment vs. rotation hysteresis loops of the west column for cycles 34, 42 and 47. The moments plotted in the figure are those extrapolated from the strain gage readings of the beam. They are determined with respect to the center of the beam-to-column connection. The rotations are the values obtained from the rotation gages mounted at a distance 1 in. above and below the horizontal stiffeners. These loops also have a curved shape, but are generally not symmetrical because the moments are not equal for

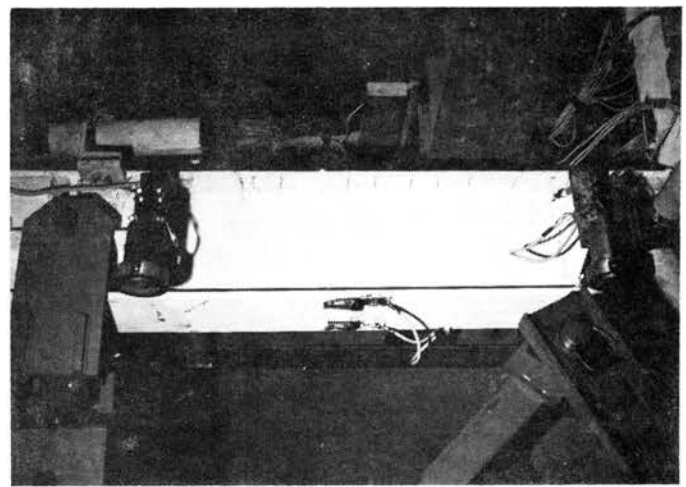


FIGURE 4.4. Spread of yielding in beam of Frame A

two equal lateral displacements applied at the column tops.

Figure 4.5 shows the significant shear yielding and distortions in the panel zones of the beam-to-column connections. Close examinations of the connections show that the distortion was more extensive in the panel zone stiffened by diagonal stiffener. In spite of the extensive yielding of the panel zones, both the diagonally stiffened connection and the doubler connection were capable of transmitting a bending moment in excess of the plastic moment of the beam. Near the end of the test, small cracks were observed in the welds at the upper end of the diagonal stiffeners.

### 4.3 Three-Story Frame B

Fifty-four cycles at various amplitudes of lateral displacements were applied to Frame B with a maximum cycled amplitude of 10 in. The largest cycled displacement was about 9 times the displacement at working load.

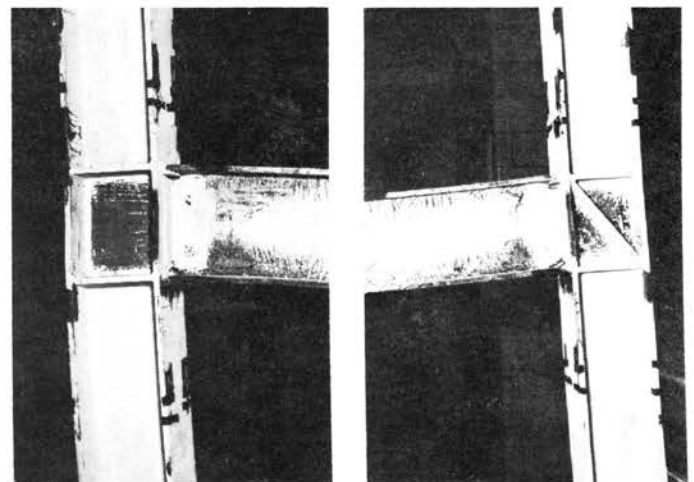


FIGURE 4.5. Beam-to-column connections of Frame A after testing

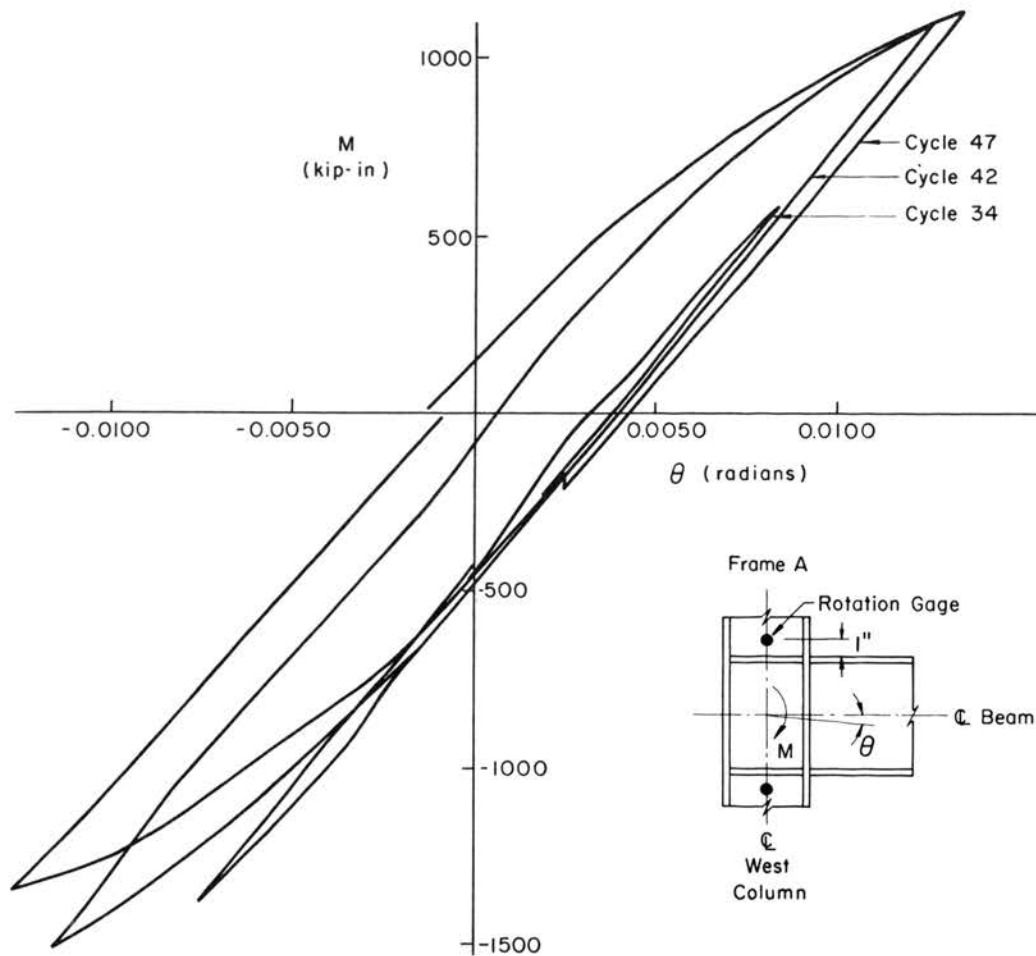


FIGURE 4.6. Moment vs. rotation hysteresis loops of west column of Frame A

After alignment of the columns had been completed, the dead load portion of the total working gravity load was applied to the beams and columns. Several cycles of displacement amplitudes in the elastic range were applied to check out the testing arrangement.

The total gravity load applied to each load point of the beams was also 17.3 kips and that applied to the top of each column was 69.1 kips.

The nominal lateral displacement program was then applied to the top of the three-story frame. The particular program consisted of three cycles at amplitudes of 1.0 and 2.0 in. (cycles 5 through 10). Then five cycles were applied at amplitudes of 3.0, 4.0, 5.0, 6.0 (6 cycles), 7.0, 8.0, 9.0 and 10.0 in. (cycles 11 through 51). After the five cycles at 10.0 in. were completed, the gravity loads on beams and columns were reduced to the dead load portion of the total working gravity loads and two additional cycles were applied at an amplitude of 10.0 in. (cycles 52 and 53). The test was continued by reestablishing the full working gravity loads on the beams and columns. The test was stopped after displacing the top of the frame to

about 13.5 in. to the east. The displacement program adopted for this test is shown in Figure 4.7.

The hysteresis loops for selected displacement amplitudes for the frame are indicated in Figure

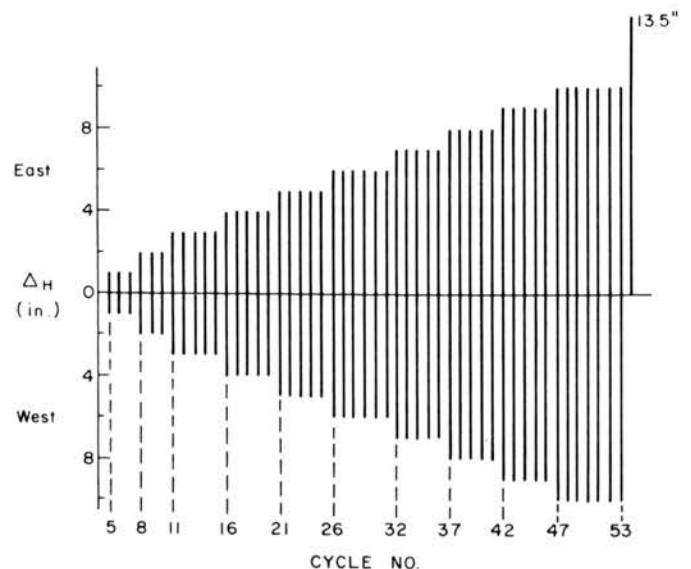


FIGURE 4.7. Displacement program for Frame B

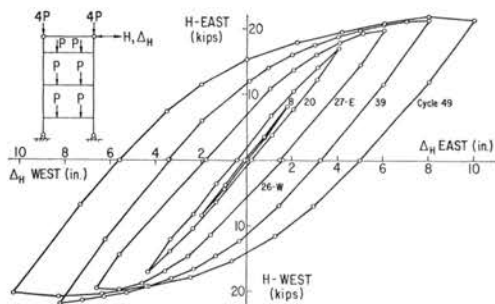


FIGURE 4.8. Selected load vs. deflection curves for Frame B

4.8. The maximum lateral load attained during the test was also about 40% greater than the maximum load predicted for the monotonic loading.

The hysteresis loops repeated at all the displacement amplitudes were stable also for this taller frame. The downward sloping portion after maximum load had been reached was also more gentle as was the case for Frame A.

The hysteresis loops for the two 10-in. cycles involving reduced gravity loads (cycles 52 and 53) are identical to those obtained when the beams and columns were loaded with full gravity loads. The loop for cycle 52 (not illustrated) duplicates closely the loop shown in Figure 4.8 for cycle 49.

As in Frame A, yielding occurred primarily in the beams and connections. Yield lines extended along the beams between the load points and the connections (Fig. 4.9). The compression flanges of the beams eventually buckled laterally. Figure 4.10 shows a top view of the buckled flange near the west end of the second story beam. The buckling of the flanges did not seem to affect the stable characteristics of the hysteresis loops, because all the loops of the last seven cycles of testing (amplitude = 10 in.) are almost identical.

The shear yielding and distortion of the beam-to-column connections can be seen in Figure 4.9. These connections performed satisfactorily during the test, they were able to resist bending moments larger than the plastic moment of the W10×29 beam.

#### 4.4 Single-Story Frame C with Noncompact Beam

Seventy cycles at various amplitudes of lateral displacements were applied to Frame C with a maximum displacement amplitude of 5.2 in. The largest cycled displacement was about 14 times the deflection at the working value of lateral load.

The basic gravity loads applied to the test frame during the main portion of the test were 17.3 kips at each load point (at 0.275 L from the center of

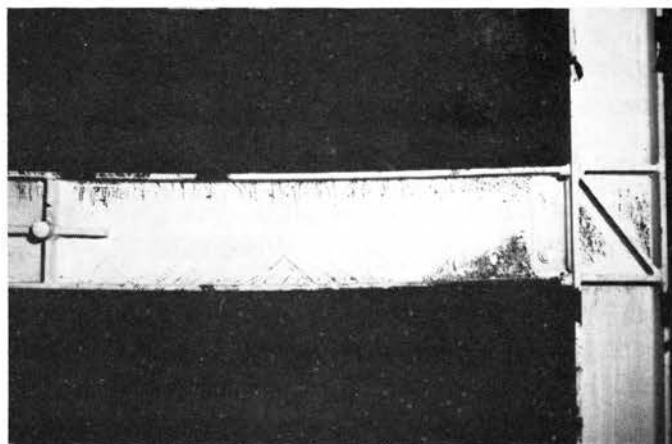
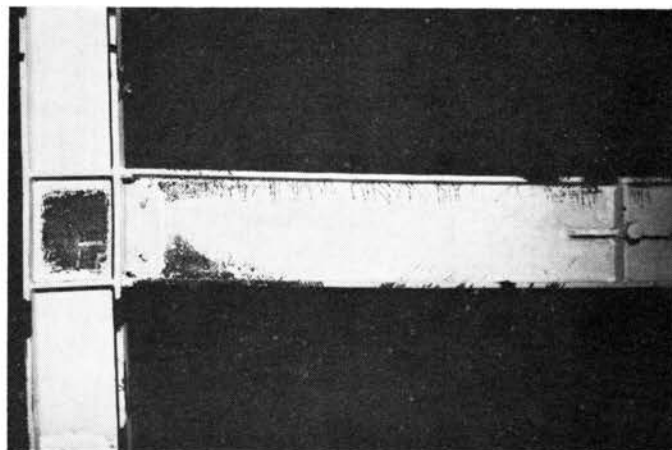


FIGURE 4.9. Spread of yielding in beam of Frame B

each column) and a total of 103.8 kips applied to the top of each column.

The lateral displacement program, which is similar to the program adopted for Frame A, consisted of three cycles at amplitudes of 0.2, 0.4 and 0.6 in. Then five cycles were applied at amplitudes of 0.8, 1.1, 1.4, 1.7, 1.9, 2.2, 2.3, 3.3, 4.0, 4.6 and 5.2 in. Five additional cycles were then applied at 5.2 in. to investigate various conditions in the beam-to-column connections and the panel zones. The test was stopped after displacing the frame to the west to 11.8 in. and then removing all loads. The entire displacement program adopted in testing this frame is summarized in Figure 4.11.

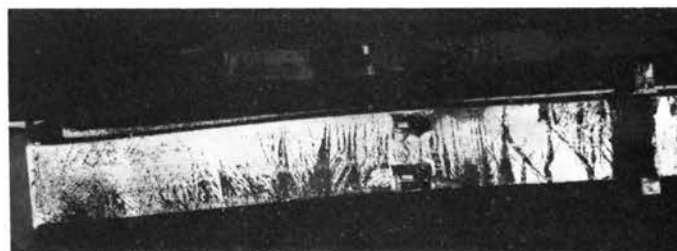


FIGURE 4.10. Lateral buckling of second story beam of Frame B

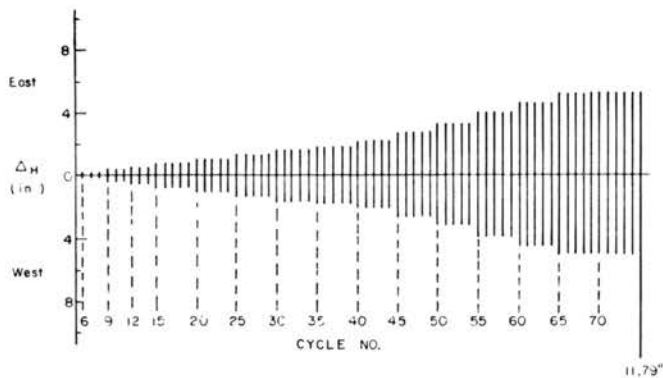


FIGURE 4.11. Displacement program for Frame C

As described in Section 2.3, Frame C is essentially a duplicate of Frame A except that the beam flanges have a  $b/t$  ratio of 21. The  $W8 \times 40$  columns for both frames A and C were from the same length of steel. The beam of Frame C was welded from selected plate stock which had approximately the same static yield stress level as the flanges of the rolled beam used in Frame A. The depth of the welded section was also 10 in., but its flange width was adjusted to give nearly the same full plastic moment and elastic section modulus as the experimental properties of the  $W10 \times 29$  beam. The experimental properties for the beams used in Frames A and C show that Frame C is slightly stronger and stiffer (Table I).

TABLE I. Comparison of Frames A and C

Frame	Moment of inertia, $I_z$ ( $in.^4$ )	Section modulus, $S_z$ ( $in.^3$ )	Plastic moment, $M_p$ ( $kip-in.$ )	Theoretical max. load, $*H_{max}$ (kips)
A	166.9	32.2	1301	15.5
C	178.7	34.3	1349	17.2

\* Determined using experimental properties for monotonic loading condition.

Selected load-deflection curves for Frame C are shown in Figure 4.12 for amplitudes of 2.2, 2.8 and

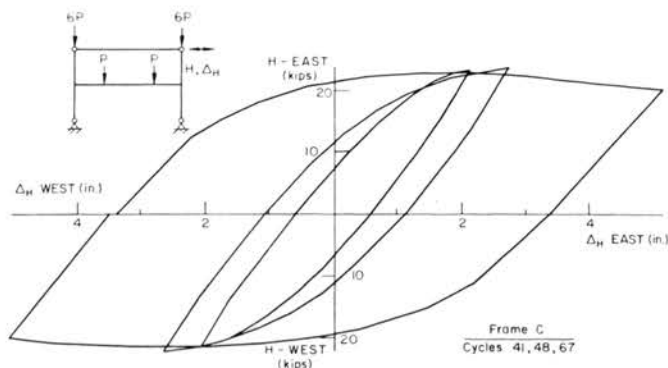


FIGURE 4.12. Selected load vs. deflection curves for Frame C

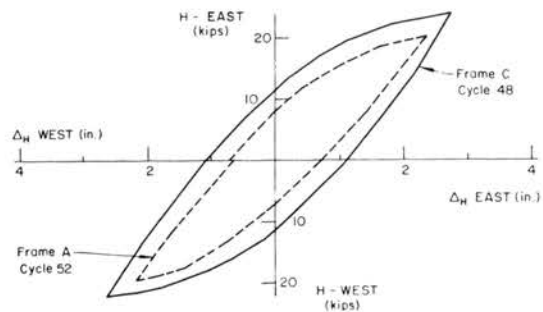


FIGURE 4.13. Comparison of load vs. deflection curves for Frame A and Frame C (small displacement amplitudes)

5.2 in. Local buckling did occur in the beam flanges at relatively early stages of testing. However the hysteresis loops are apparently unaltered by the flange buckling. This is illustrated in Figures 4.13 and 4.14 where hysteresis loops of Frames A and C are compared for two approximately equal lateral displacements. The maximum lateral loads obtained for similar amplitudes of displacement of the two frames are shown in Table II.

TABLE II. Experimental Maximum Loads of Frames A and C

Frame	Nominal displacement amplitudes (in.)		
	$\pm 2.2$	$\pm 2.8$	$\pm 5.2$
	Max. load obtained from test (kips)		
A	19.1	20.0	21.2
C	22.6	23.2	22.5

The maximum loads are consistently higher for Frame C, even with extensive local buckling occurring in the beam (Fig. 4.15). The relative differences between Frames A and C are slightly larger than the differences expected due to the differences in the beam properties.

Near the termination of the original test plan (cycle 69), fracture of the beam flange occurred.

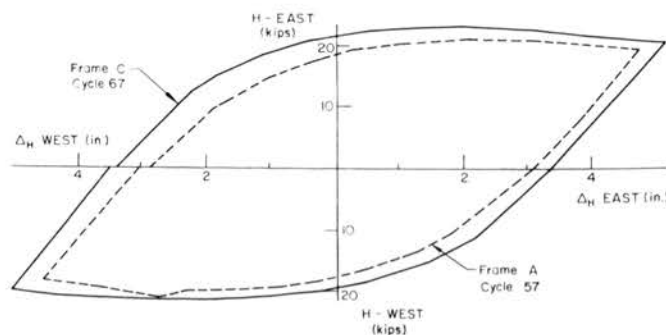


FIGURE 4.14. Comparison of load vs. deflection curves for Frame A and Frame C (large displacement amplitudes)

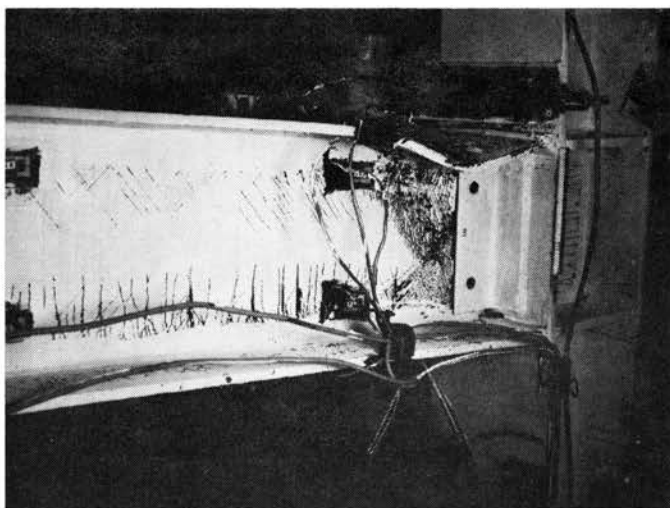


FIGURE 4.15. Flange local buckling in beam of Frame C

At this point, the frame was repaired and additional testing was performed to study the following two problems:

1. The necessity for placing shear stiffening in the panel zone of the beam-to-column connections.
2. The necessity for welding the beam web to the column flange.

Figure 4.16 shows the effect of removing the shear stiffeners. There is a definite decrease in the stiffness and also a drop in the maximum load, but the general shape of the hysteresis loops is not significantly changed.

The next step in the testing was to cut the web of the beam free of the column. The two erection bolts ( $\frac{3}{4}$  in. diameter) were inserted between the web and the erection clip angle (refer to Fig. 4.15 for a view of the east connection with the erection bolts removed). The resulting behavior, as shown by the solid curve in Figure 4.17, is essentially the same as when the web was fully welded.

For a more conclusive comparison, the shear stiffeners were replaced in the panel zone. Again

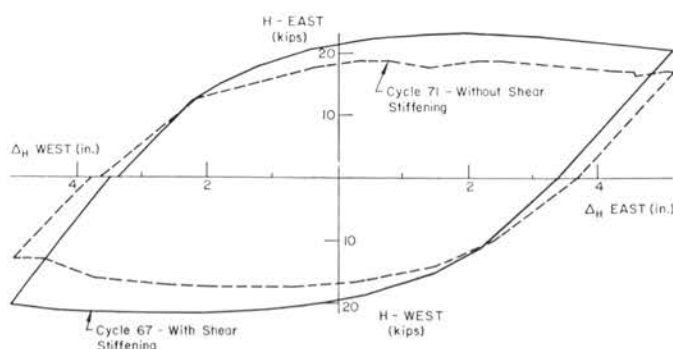


FIGURE 4.16. Effect of removing shear stiffening in Frame C

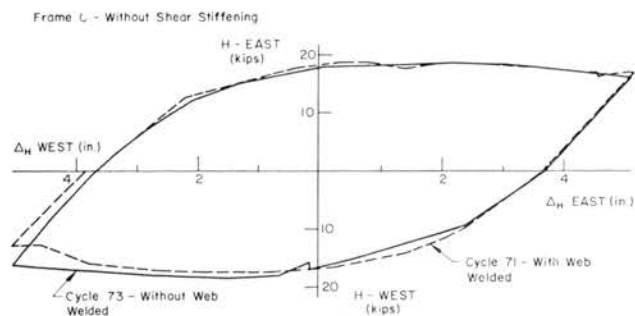


FIGURE 4.17. Effect of a bolted web and shear stiffening removal in Frame C

the effect of having the web welded to the column flange or not is still apparently small, as shown by the dashed curve in Figure 4.18.

Figure 4.19 shows the flange buckles developed in the beam and the shear distortion of the beam-to-column connections. The shear distortions in these connections are more extensive than those in the connections of Frames A and B. This is because of the larger bending moment acting at the connections in Frame C. The connection stiffened by doubler plates suffered less shear distortion than the diagonally stiffened connection.

#### 4.5 Single-Story Frame D with Minor Axis Column Orientation

Sixty-nine cycles at various amplitudes of lateral displacements were applied to Frame D with a maximum displacement amplitude of 5.2 in. The largest cycled displacement is about 14 times the deflection at the working value of lateral load.

The basic gravity loads applied to the test frame during the main portion of the test were 17.3 kips at each load point (at 0.275 L from the center of each column) and a total of 103.8 kips applied to the top of each column.

The lateral displacement program consisted of three cycles at amplitudes of 0.2, 0.4 and 0.6 in. Then five cycles were applied at amplitudes of 0.8, 1.1, 1.4, 1.7, 1.9, 2.2, 2.8, 3.3 (10 cycles),

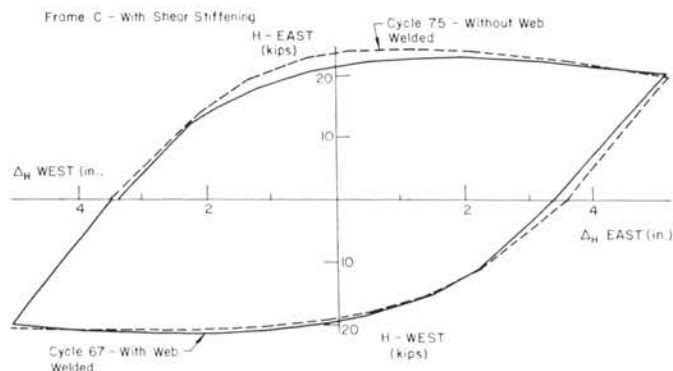


FIGURE 4.18. Effect of a bolted web in Frame C

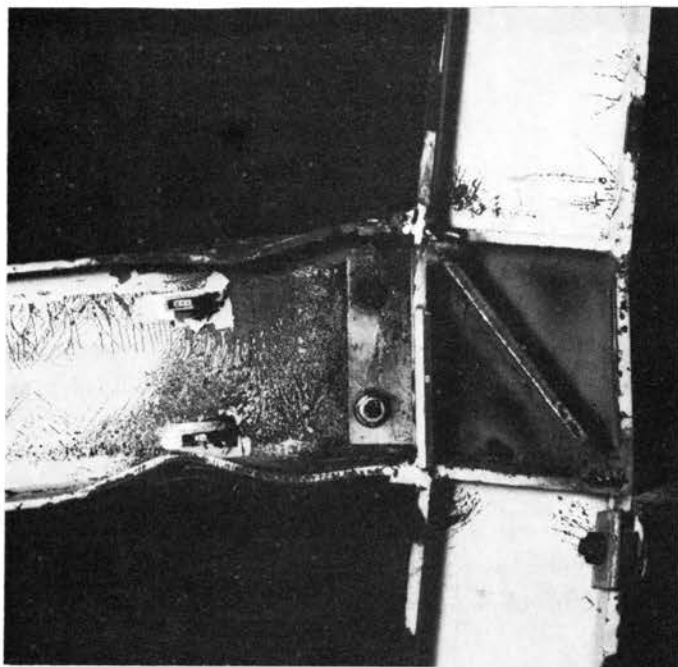
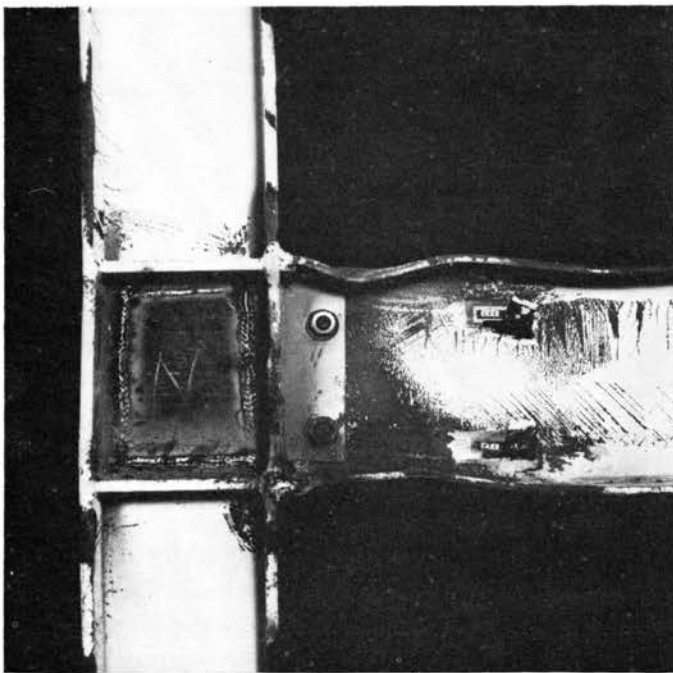


FIGURE 4.19. Flange buckling in beam of Frame C

4.0, 4.6 and 5.2 in. The displacement program adopted for this frame is similar to the basic program used for Frames A and C and is shown in Figure 4.20.

As can be observed in Figure 4.21, the load vs. deflection hysteresis loops at the 2.8-in. amplitude show the same stability as the previous tests even though the columns were partially yielded. Figure 4.22 shows the yield lines in the beams, columns and connections. Both columns were exten-

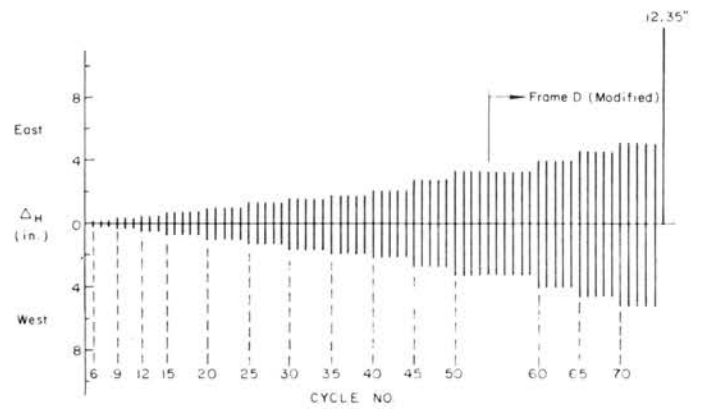


FIGURE 4.20. Displacement program for Frame D

sively yielded near the connections due to the combined influence of axial thrust and bending moment. However, they remained essentially straight and bent in double curvature during the application of all the 2.8-in. displacement cycles.

During the 3.3-in. amplitude cycling the general behavior of the columns changed from double curvature to single curvature bending and the hysteresis loops obtained did not show the same degree of repeatability (Fig. 4.23). Eventually, the entire frame could not be pulled back any more. This was due to the very large  $P-\Delta$  moments accumulated in the severely bent columns as can be observed in Figure 4.24. At this stage the columns were straightened and reinforced by cover plates. These plates were welded to the flange tips of the columns above and below the connections. This alteration was completed before starting cycle 54. At the end of the test the frame was displaced to the east to about 12.4 in.

The hysteresis loops obtained for the 3.3 (after reinforcing), and 5.2-in. amplitude cycling are shown in Figures 4.25 and 4.26. The hysteresis loops of Figure 4.25 are comparable with those of Figure 4.21. The general shape of the loops is

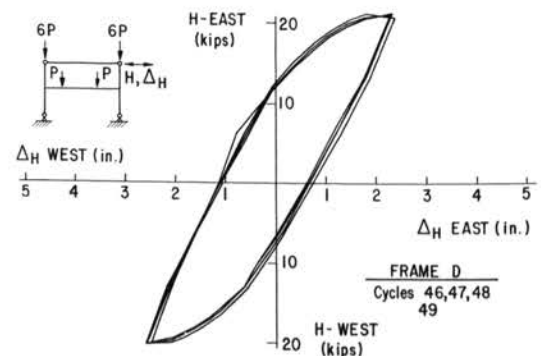


FIGURE 4.21. Load vs. deflection curves of Frame D ( $\pm 2.8$  in. nominal displacement)

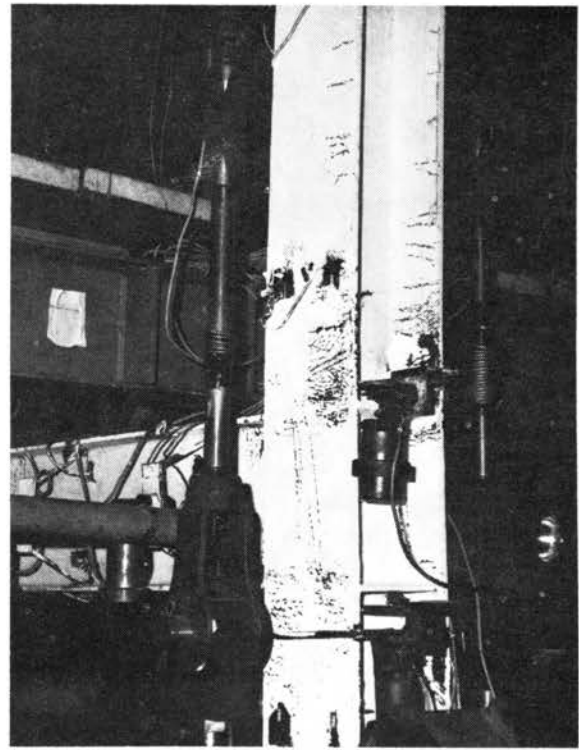
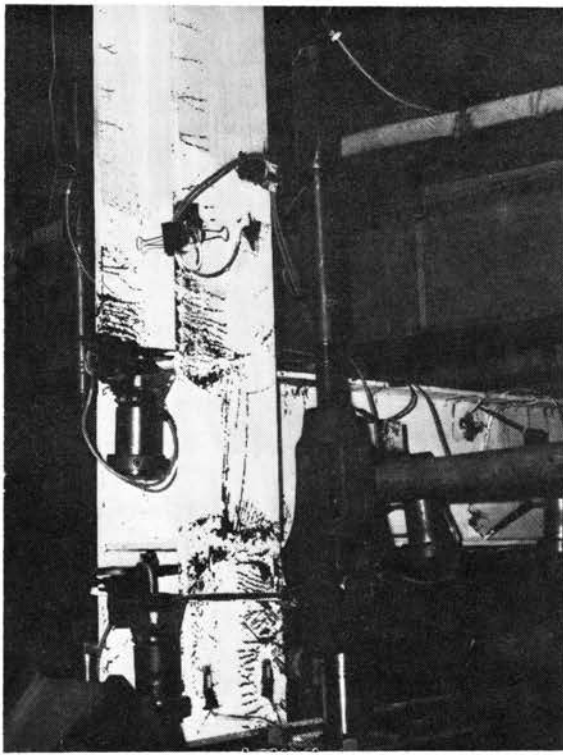


FIGURE 4.22. Yielding in beam, columns and connections of Frame D

similar, but the maximum lateral loads are different. Because of the added cover plates, the frame was substantially stronger and therefore a higher maximum load was obtained. The hysteresis loops of all the cycles performed after reinforcing the columns are stable and do not change from cycle to cycle.

#### 4.6 Two-Story Frame E with Hinges in Columns and Beams

As mentioned in Section 2.5, Frame E was designed specifically to study the behavior of columns with plastic hinges forming at the two ends. Lateral bracing was provided only at the floor levels and at the column tops. The theoretical analysis given in Figure 2.11 indicates that the

hinges would form at both ends of the middle columns. These columns were the critical elements in the frame and were expected to fail by inelastic lateral-torsional buckling.

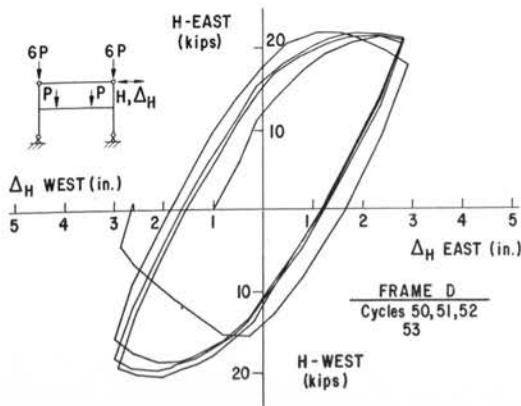


FIGURE 4.23. Load vs. deflection curves of Frame D ( $\pm 3.3$  in. nominal displacement)

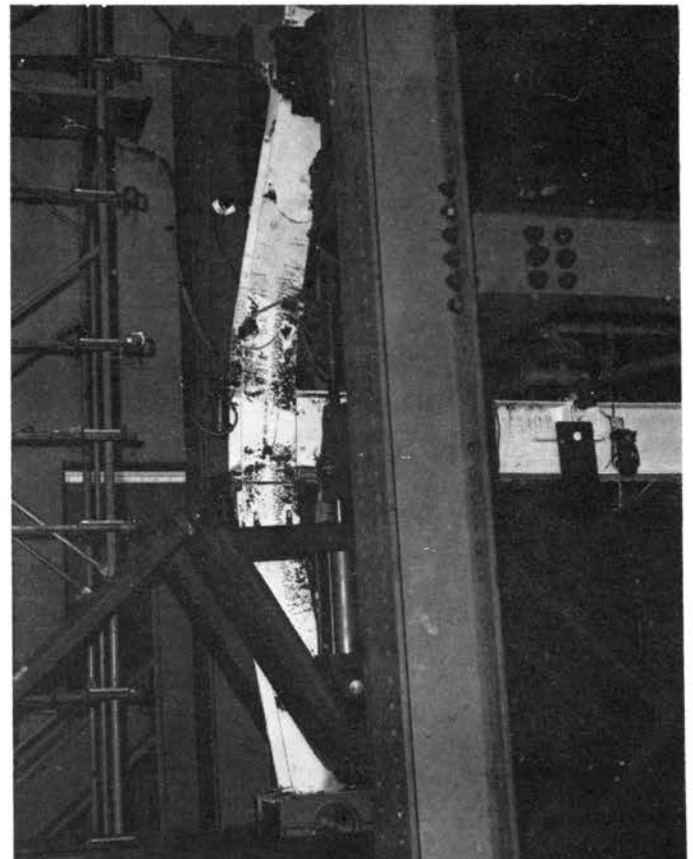


FIGURE 4.24. Severely bent column in Frame D

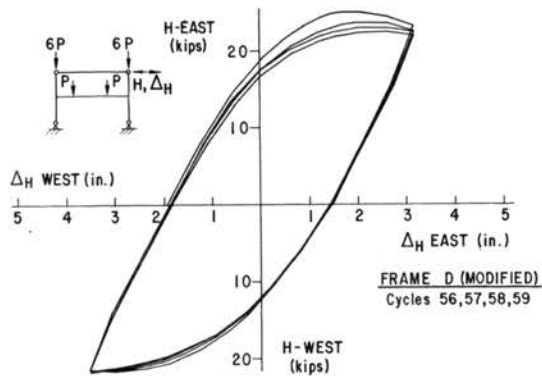


FIGURE 4.25. Load vs. deflection curves of Frame D (modified) ( $\pm 3.3$  in. nominal displacement)

The gravity loads that were applied to the frame and maintained throughout the test were 17.3 kips in the beams and 86.4 kips at the column tops. The axial load ratio,  $P/P_y$  in the middle columns is equal to 0.41 which is substantially higher than those in the other four frames. The columns were aligned under a set of gravity loads equal to about half of the total values.

Thirty-nine cycles of controlled lateral displacements were applied to the frame with a maximum amplitude of 6 in. The displacement program consisted of three cycles at amplitudes of 0.4 and 0.8 in. and five cycles at 1.20, 1.50, 2.0 (6 cycles), 3.0, 4.0, 5.0 and 6.0 (one cycle only) in. The frame behaved satisfactorily during the first cycle of the 6-in. displacement, but failed (unable to reach the previously established maximum load) in the subsequent cycle. The actual displacement program followed during the test is given in Figure 4.27.

Figure 4.28 shows the hysteresis loops for several selected displacement amplitudes. The maximum load observed is 21.9 kips which is about 17% above the computed maximum load for the monotonic loading condition. Visible yielding of the column ends and the panel zones of the connections

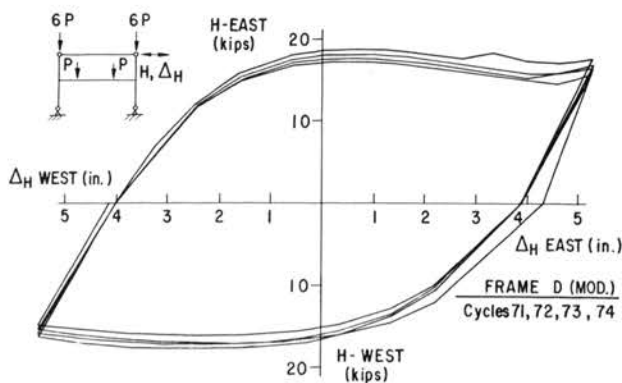


FIGURE 4.26. Load vs. deflection curves of Frame D (modified) ( $\pm 5.2$  in. nominal displacement)

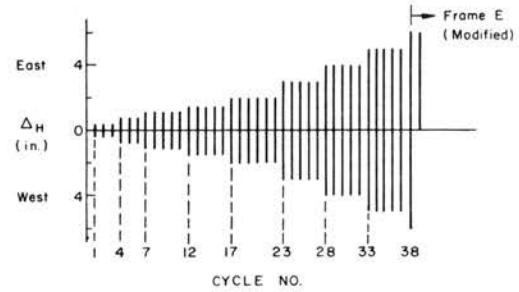


FIGURE 4.27. Displacement program for Frame E

occurred after the first two cycles of 1.20-in. displacement. Yielding progressed rapidly in the middle and upper columns during the subsequent cycles, but no lateral or torsional deformation was apparent in the columns.

After the third 3-in. cycle, the upper and middle columns on the east side buckled suddenly like a single column about their minor axis. The frame was unloaded and an extra brace was added near the lower end of the top column. The frame was realigned and the test was continued. The hysteresis loops obtained before (cycles 24 and 25) and after (cycles 26 and 27) this adjustment are given in Figure 4.29.

During the second cycle of the 4-in. displacement local buckling of the inner flanges near the upper ends of the middle columns became visible. Yielding has spread extensively in the columns. The same situation also developed in the upper columns. However, the overall stability of the frame was not significantly affected and the test was continued. Twisting, together with out-of-plane deformation of the middle columns, occurred during the application of the first 5-in. displacement cycle. The combined effect of local buckling and lateral-torsional buckling caused the middle column to distort extensively. During the last

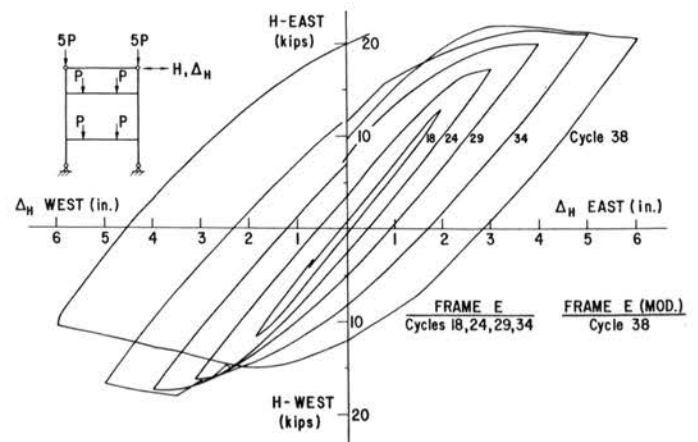


FIGURE 4.28. Selected load vs. deflection curves of Frame E and Frame E (modified)



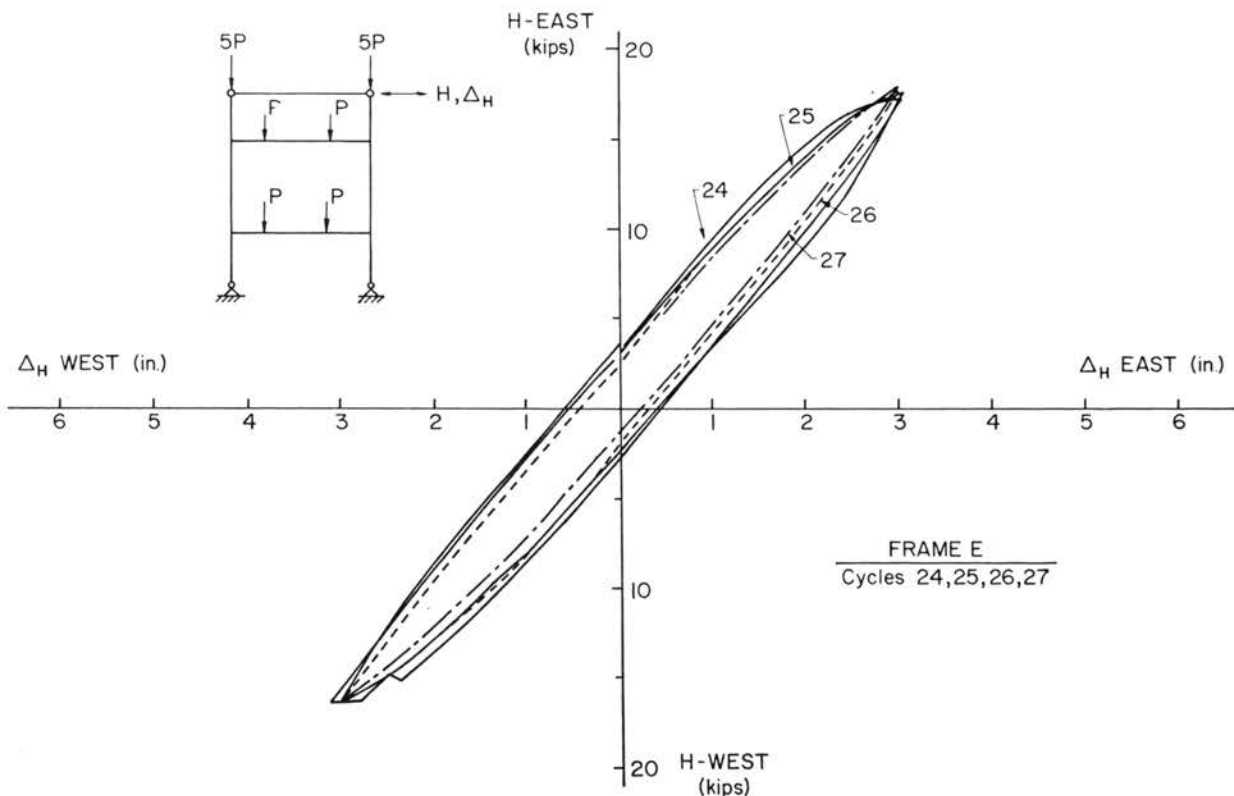


FIGURE 4.29. Load vs. deflection curves of Frame E ( $\pm 3.0$  in. nominal displacement)

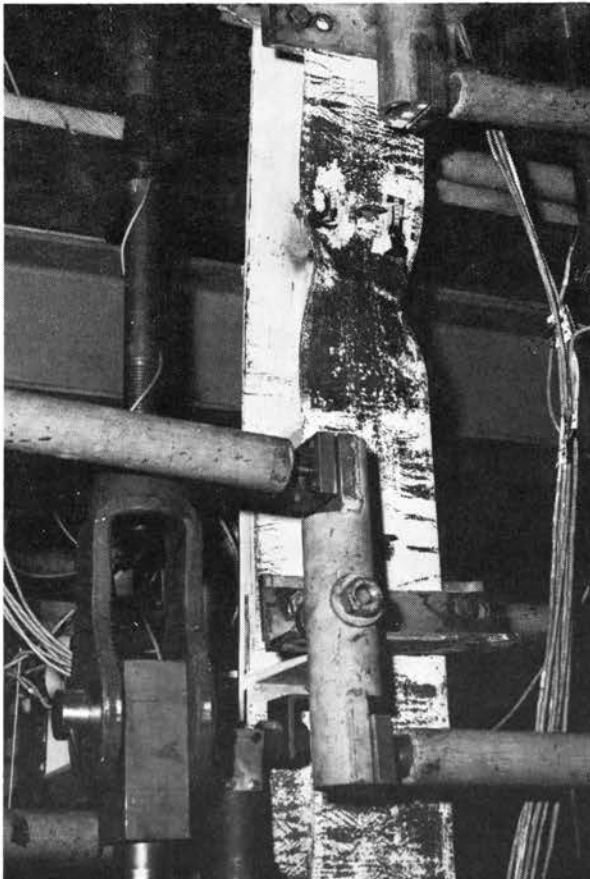


FIGURE 4.30. Severe local buckling in upper column of Frame E

of the 5-in. cycles local buckling of the upper column (east) became so severe that the gravity loads at the column tops could no longer be maintained. The severe local buckling is shown in Figure 4.30.

The frame was unloaded again and cover plates ( $\frac{1}{4} \times 6 \times 14$  in.) were welded to flanges (on the less distorted side) of the upper columns. This was done in order to force failure in the middle story. The first cycle with a 6-in. maximum displacement was then applied which resulted in very extensive distortions of the two middle columns. Finally, it became impossible to displace the frame to the 6-in. displacement without a drop in the applied gravity loads. The test was stopped after the second attempt to repeat the 6-in. hysteresis loops had failed. Figure 4.31 shows the lateral and torsional distortion and the spread of yielding near the plastic hinges of the west column. The deformed configuration of the entire frame is shown in Figure 4.32.

## 5. Observations Based on Experimental Results

### 5.1 Comparison of Maximum Experimental Loads with Predicted Loads for Monotonic Loading Condition

A considerable increase in lateral load capacity is possible for frames subjected to conditions

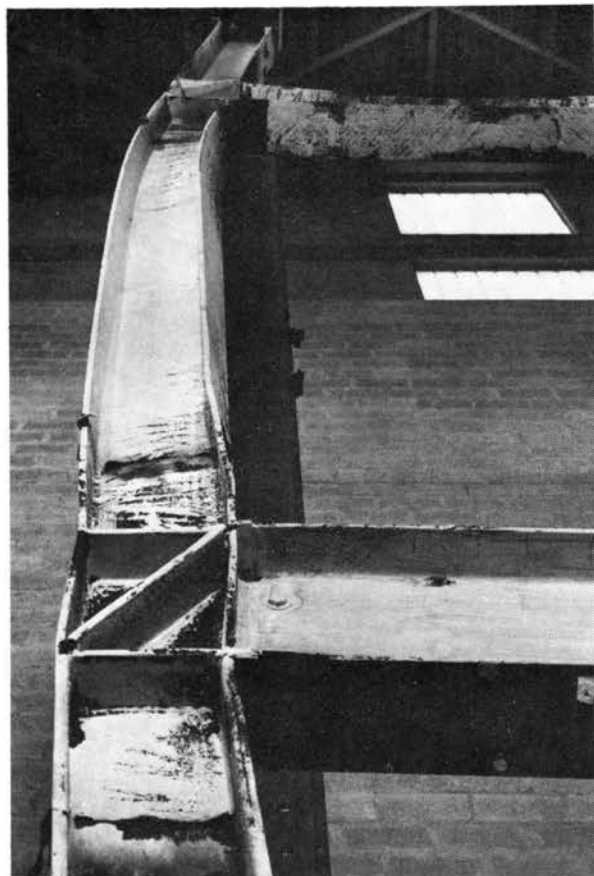


FIGURE 4.31. Lateral and torsional distortion in middle column of Frame E

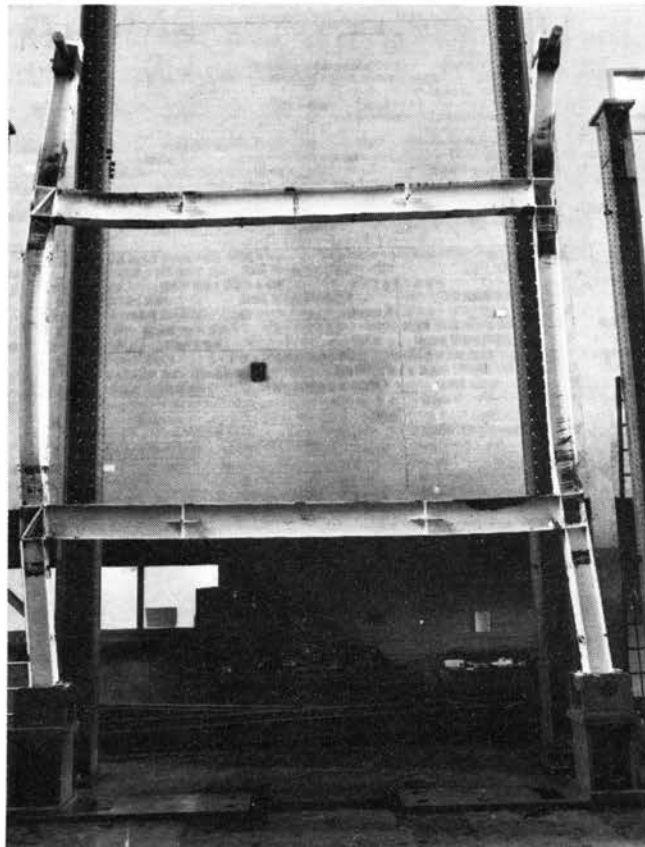


FIGURE 4.32. Frame E after testing

similar to those existing in the experimental program. The frames tested in the program were single-bay in width and were subjected to constant gravity loads on the beams and on the column tops. The ratios of the maximum applied axial load to the axial yield load of the columns varied from 0.25 to 0.47. The frames were braced to prevent out-of-plane movements of the beams. The horizontal displacement program should be noted since other programs would change the resulting frame behavior (Figs. 4.1, 4.7, 4.11, 4.20 and 4.27).

For Frames A, B and C a 40% increase in the maximum lateral load was observed. The increases for Frames D and E were about 30 and 17%, respectively. These increases were based on comparisons with the predicted maximum loads for the monotonic loading condition. The effect of strain hardening was not included in the predictions.

### 5.2 Stability of the Hysteresis Loops

The experimental results presented in Chapter 4 show the stability of the hysteresis loops during the repetitions of cycles at each amplitude. The curves seem to have equal stability for amplitudes which are less than or greater than those at which the maximum lateral load occurs.

During the test of Frame C, where the load was expected to vary because of the influence of local buckling, most of the loops remained stable. Only in one set of cycles during which the diagonal stiffening weld was breaking did the load decrease.

During the test of Frame D, after the columns were partially yielded, the hysteresis loops of the 3.3-in. amplitude cycles began to distort while deformed configurations of the columns changed from double to single curvature (Fig. 4.23).

The hysteresis loops of Frame E remained stable even after the columns have deflected noticeably in the out-of-plane direction. The formation of the plastic hinges at the ends of the columns did not affect the lateral stability of the columns. However, the overall structure appeared to be stable and was able to undergo significant inelastic deformations in the direction of the applied load. The hysteresis loops began to deteriorate only after the center portions of the columns had twisted and deflected very substantially.

### 5.3 Shape of Hysteresis Loops

The experimental curves presented show the curvilinear nature of the load vs. deflection relationship. The shape of the hysteresis loops is

affected by the reduction of member and frame stiffness during the reversed and repeated loading. The spread of yielding at the plastic hinge locations as well as the Bauschinger effect in the material itself are contributing factors. Nonlinear strain distributions at a cross section, nonlinear stress vs. strain characteristics, effect of axial strains and the  $P-\Delta$  moments existing throughout the frame are additional factors which influence the shape of the hysteresis loops.

The role of strain hardening can be observed by comparing the unloading slope beyond the maximum loading computed for the monotonic loading case with the similar slope indicated in the tests. Apparently the experimental slope is about  $\frac{1}{3}$  of that indicated in the elastic-plastic analysis without strain hardening. This contributes to the energy-absorbing capacity of the ductile frames.

#### 5.4 Connection Details

All connections performed adequately during the tests. The maximum moment applied to the connections exceeded the plastic moment of the beams by about 10 to 20%. For Frames A, B and C the weld between the diagonal stiffener and column flange became inadequate only after extensive yielding had already occurred in the connections. The stiffener plate sizes and welds to the column webs performed satisfactorily. The doubler plated panel zones performed well throughout the tests even with extensive yielding in the later portions of the tests.

The possibility of low cycle fatigue was indicated by fracture near the flange welds of the beam-to-column connections of Frame C. This fracture occurred several times in the last few cycles of the test.

The addendum to the test of Frame C also indicated that shear stiffening of the panel zones of the test frame helped to increase the maximum lateral load (Fig. 4.16). It should be possible to allow for the effect of connection distortion in design calculations if the expense of providing shear stiffening is to be avoided.

The test results of Frame C also gave an indication that no significant change in lateral capacity of the frame would be found if the beam webs were bolted to the column flange instead of welding (Figs. 4.17 and 4.18). Apparently, whether the panel zone is stiffened or not does not affect this conclusion.

The minor axis beam-to-column connections used for Frame D had no apparent deficiencies.

#### 5.5 Behavior of Frames with Noncompact Beams

Based on the behavior indicated by the single test of Frame C, local flange buckling in a beam does not affect the behavior of the frame. The load vs. deflection hysteresis loops for Frame C were stable in both size and shape at each deformation amplitude. The nominally critical  $b/t$  ratio for the A36 steel is about 17 based on earlier studies for monotonic loading. The result of this test indicates that a somewhat higher limiting  $b/t$  ratio could be permitted for beams in building frames.

The local buckling of the beam flanges during equal amplitude cycling of the frame did not occur and disappear alternately. The alternating buckling and complete straightening could not occur since gravity loads were also on the beam. Therefore, the completely reversed conditions which have been evaluated previously in cantilever beam tests should be examined carefully when applied to frames subjected to combined gravity and lateral loads.

#### 5.6 Behavior of Frames with Columns Orientated for Minor Axis Bending

As evidenced by Frame D, no particular problems will occur due to the column orientation if the yielding is constrained to be in the beam only. However, for columns with moments appreciably exceeding the minor axis yield moment and approaching the fully plastic moment, the elastic-plastic analysis is not completely suitable to define the frame response.

#### 5.7 Behavior of Frames with Plastic Hinges in Columns and Beams

The general behavior of Frame E is not significantly different from that of the other four frames. The formation of plastic hinges in the columns did not seem to change the shape of the hysteresis loops. The bending moment values measured during the test indicate that strain hardening also occurred in the yielded zones of the columns. The effect of strain hardening on the bending moment is consistent with the observations made previously from the results of a series of tests of beam-and-column subassemblages (40). The response that led to the eventual failure of the frame is inelastic lateral-torsional buckling. The torsional deformation caused by buckling tends to increase significantly under repeated applications of the lateral load.

## 6. Summary and Conclusions

A series of tests on five full-scale steel frames subjected to constant gravity loads and repeated and reversed lateral displacements has been described. The loads assumed in the design of the test frames were based on the current aseismic design requirements as applied to an eight-story single-bay structure (Fig. 2.2). The member sizes of the first two frames (single-story Frame A and three-story Frame B) were selected based on the weak-beam, strong-column concept and were checked to satisfy the allowable-stresses specified in the AISC Specification. Elastic-plastic analyses were performed on these frames for the monotonically increasing lateral loading condition in order to evaluate the behavior and maximum strength in the inelastic range. The results of the analyses also assured that no plastic hinges would form in the members under working loads.

The third frame (Frame C) was essentially a duplicate of Frame A except that the beam of this frame had a width-to-thickness ratio exceeding the limiting value specified in Part 2 of the AISC Specification. The purpose of this noncompact beam test was to investigate the effect of inelastic local buckling on the hysteretic behavior.

The fourth frame (Frame D), was designed to study the behavior of frames with columns orientated for minor axis bending. The columns, as well as the beams, were yielded extensively during the test.

The behavior of frames designed based on the strong-beam, weak-column concept was investigated with the fifth frame (Frame E). The member sizes of this frame were so selected that plastic hinges would form first in the columns.

The beam-to-column connections were designed as fully moment resisting and are similar to those tested by Popov (18). In addition, the panel zones were provided with shear stiffening (diagonal stiffeners or doubler plates) in accordance with the requirements of the AISC Specification.

In a building, the floor system would provide lateral support to both beams and columns. Hence, the beams in the test frames were braced at the top flanges against out-of-plane movement. Lateral braces were attached in pairs to the columns at the floor levels. These braces prevented both the lateral and torsional deformations of the columns.

Based on the results obtained from this investigation the following conclusions may be reached:

1. Steel frames with fully welded moment-resisting connections are very ductile and can undergo large inelastic deformations, as much as 14 times the lateral working load deflection, when subjected to repeated and reversed lateral displacements. For Frames A, C, and D, this corresponds to a nominal drift index of  $5.2/120 = 0.043$  in those tests.

2. The maximum load-carrying capacity of a steel frame under repeated lateral displacement can be substantially higher than that under monotonic loading. This is due primarily to the effect of the  $P-\Delta$  moment (44).

3. The presence of the  $P-\Delta$  moment affects the overall stability of a frame. For large displacement cycles, the hysteresis loops tend to reach a maximum beyond which the lateral load decreases in order to maintain equilibrium.

4. The lateral load vs. deflection hysteresis loops corresponding to a constant maximum displacement are highly reproducible. This holds true even for displacements far greater than those corresponding to the maximum load.

5. The shape of the hysteresis loops is affected by the reduction of frame stiffness caused by yielding and by the Bauschinger effect in the material.

6. Strain hardening plays an important role in frame response for displacements greater than those corresponding to the maximum load. In this displacement range, strain hardening increases the lateral load that is resisted and the energy that is dissipated in repeated displacement cycles.

7. Strain hardening also increases the moment resisted at the ends of beams by about 10 to 20%. The connections transmitted these increased and repeatedly applied beams moments in spite of the fact that plastic beam moments were used to design the connections.

8. The results of Frame C indicate that the occurrence of beam flange buckling in noncompact beams does not change significantly the shape and the reproducibility of the hysteresis loops. However, the flange buckles tend to introduce high local stresses in the beams near the connections. A flange fracture occurred at this location during cycle 69 with a drift index of 0.043.

9. The results of Frame C also indicate that the lateral load capacity of a steel frame may be reduced when shear stiffening is removed from the panel zones of the beam-to-column connections. The ductile and reproducible behavior of the frame, however, appears to be unaffected.

10. A comparison of the results obtained from Frames A and D shows that the hysteretic behavior of a frame is not changed by orientating its columns for minor axis bending. No major differences in the characteristics of the hysteresis loops was observed during the test of Frame D for a nominal drift index of  $2.8/120 = 0.023$  in spite of minor axis column moments appreciably larger than the yield moment.

11. The formation of plastic hinges in the columns does not result in any immediate change of the hysteretic behavior of a frame, as illustrated by the results of Frame E test. However, if the columns are not adequately braced in the perpendicular direction, lateral-torsional buckling may eventually cause failure of the columns under large repeated lateral displacement cycles.

Finally, it should be emphasized that the last four conclusions are based on the test results presented in this report. Further research would be useful to fully verify these observations.

## 7. References

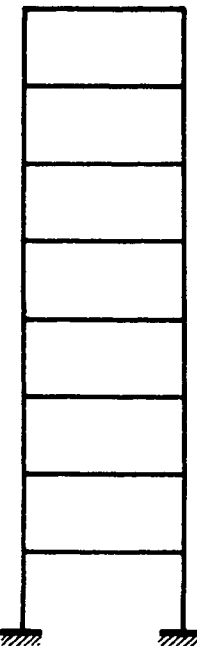
1. International Conference of Building Officials, "Uniform Building Code" (in particular sections 2314, 2722, 2723), Pasadena, Calif., 1970.
2. Sfantescio, D., "Dynamic Effects of Wind and Earthquake," Theme IIIc, Preliminary Publication of IABSE, Eighth Congress, New York, Sept. 1968 (Pub. June 1967).
3. Hanson, R. E., "Comparison of Static and Dynamic Hysteresis Curves," *Journal of the Engineering Mechanics Division, ASCE*, 92 (EMS), p. 87, Oct. 1966.
4. AlMutl, A. M., "Post-Elastic Response of Mild Steel Beams to Static and Dynamic Loading," Ph.D. Dissertation, The University of Michigan, June 1970.
5. Manjoine, M. J., "Influence of Rate of Strain and Temperature on Yield Stresses of Mild Steel," *Transactions, ASME*, Vol. 66, 1944, pp. A211-218.
6. Rao, N. R. N., Lohrmann, M., and Tall, L., "Effect of Strain Rate on the Yield Stress of Structural Steels," *Journal of Materials, ASTM*, Vol. 1, No. 1, March 1966.
7. Benham, P. P., and Ford, H., "Low Endurance Fatigue of a Mild Steel and an Aluminum Alloy," *Journal of Mechanical Engineering Science*, Vol. 3, No. 2, June 1961.
8. Tavernelli, J. F., and Coffin, L. F., Jr., "Experimental Support for Generalized Equation Predicting Low Cycle Fatigue," *Trans. ASME*, Vol. 84, Series D, *Journal, Basic Engineering*, Dec. 1962.
9. ASCE-SRC, "Plastic Design in Steel," ASCE Manual of Engineering Practice No. 41, 1971.
10. Bertero, V. V., and Popov, E. P., "Effect of Large Alternating Strains on Steel Beams," *Journal of the Structural Division, ASCE*, 91 (ST1), p. 1, Feb. 1965.
11. Popov, E. P., and Franklin, H. A., "Steel Beam-to-Column Connections Subjected to Cyclically Reversed Loading," Steel Research for Construction, AISI, Feb. 1966.
12. Popov, E. P., and Pinkney, R. B., "Behavior of Steel Building Connections Subjected to Repeated Inelastic Strain Reversal," Experimental Data—Report No. 67-31, University of California at Berkeley, Dec. 1967, reprinted in AISI Steel Research for Construction Bulletin No. 14, Nov. 1968.
13. Popov, E. P., and Pinkney, R. B., "Behavior of Steel Connections Subjected to Repeated Inelastic Strain Reversal," Report No. 67-30, University of California at Berkeley, Dec. 1967, reprinted in AISI Steel Research for Construction Bulletin No. 13, Nov. 1968.
14. Popov, E. P., and Pinkney, R. B., "Reliability of Steel Beam-to-Column Connections under Cyclic Loading," Proceedings Fourth World Conference on Earthquake Engineering, Santiago, Chile, Jan. 1969.
15. Popov, E. P., "Performance of Steel Beams and Their Connections to Columns During Severe Cyclic Loading," Contributions to expanded discussion, Eighth Congress of IABSE, Theme III, New York, Sept. 1968.
16. Vann, W. P., Discussion of "Cyclic Yield Reversal in Steel Building Connections" by E. P. Popov and R. B. Pinkney, *Journal of the Structural Division, ASCE*, 96 (ST1), Jan. 1970.
17. Popov, E. P., "Behavior of Steel Beam-to-Column Connections under Repeated and Reversed Loading," Plastic Design of Multi-Story Frames—Guest Lectures, Fritz Engineering Laboratory Report No. 273.62, Lehigh University, July 1966.
18. Popov, E. P., and Pinkney, R. B., "Cyclic Yield Reversal in Steel Building Connections," *Journal of the Structural Division, ASCE*, 95 (ST3), p. 327, March 1969.
19. Popov, E. P., and Stephen, R. M., "Cyclic Loading of Full-Size Steel Connections," Earthquake Engineering Research Center Report No. 70-3, University of California, Berkeley, July 1970, reprinted in AISI Steel Research for Construction Bulletin No. 21, Feb. 1972.
20. Sherbourne, A. N., "Some Preliminary Experiments on the Behavior of Ductile Structures under Repeated Loads," *Experimental Mechanics*, Vol. 3, No. 5, p. 119, May 1963.
21. Krishnasamy, S., and Sherbourne, A. N., "Response of a 'Plastic Hinge' to Low Cycle Alternating Deflections," *Experimental Mechanics*, Vol. 8, No. 2, p. 133, 1966.
22. Royles, R., "Incremental Extension of Mild Steel Beams in Reversed Bending," *Journal of Strain Analysis*, Vol. 1, No. 2, p. 133, 1966.
23. Hagura, H., "Research on the Elastic-Plastic Analysis of Steel Sections Subjected to Alternative Loads," *Trans. of the Arch. Inst. of Japan*, No. 125, p. 8, July 1966.
24. Naka, T., et al., "Ultimate Strength of Columns in Multi-Story Rigid Frames," Yawata Technical Report No. 256, p. 82, Sept. 1966.
25. Naka, T., Kato, B., and Watabe, M., "Research on the Behavior of Steel Beam-to-Column Connections," Laboratory for Steel Structures, 1966, University of Tokyo, Japan.
26. Wakabayashi, M., "An Experimental Study on the Elastic-Plastic Stability of Cross Shaped Structural Systems," Kinki Branch of the Arch. Inst. of Japan, 1967.
27. Wakabayashi, M., "The Restoring Force Characteristic of Multi-Story Frames," Bulletin of the Disaster Prevention Research Institute (Japan), 14, Part 2, Feb. 1965.
28. Igarashi, S., et al., "Plastic Behavior of Steel Frames under Cyclic Loadings," *Trans. of the Arch. Inst. of Japan*, No. 130, Dec. 1966.
29. Igarashi, N. Toga, "Hysteresis Characteristics and Structural Damping of Steel Structures under Alternate Lateral Loading," *Trans. of the Arch. Inst. of Japan*, No. 120, Feb. 1960.
30. Yokoo, Y., et al., "Horizontal-Force-Restraint Properties of Multi-Story Steel Frames," Yawata Technical Report No. 256, p. 43, Sept. 1966.
31. Yarımcı, E., "Incremental Inelastic Analysis of Framed Structures and Some Experimental Verifications," Ph.D. Dissertation, Lehigh University, 1966.
32. Arnold, P., Adams, P. F., and Lu, L. W., "The Effect of Instability on the Cyclic Behavior of a Frame," Proceedings, RILEM Symposium on "Effects of Repeated Loading on Materials and Structures," Mexico City, Sept. 1966.
33. Beedle, L. S., "Reversed Loading of Frames Preliminary Tests," Proceedings, Structural Engineers Association of California, p. 87, 1965.
34. Sidebottom, O. M., and Chang, C. T., "Influence of the Bauschinger Effect on Inelastic Bending of Beams," Proceedings of First U.S. National Congress of Applied Mechanics, Vol. 1, 1952.
35. Tanabashi, R., et al., "Load-Deflection Behaviors and Plastic Fatigue of Wide-Flanged Beams Subjected to Alternating Plastic Bending," *Trans. of the Arch. Inst. of Japan*, I: No. 175, Sept. 1970; II: No. 176, Oct. 1970; III: No. 177, Nov. 1970.
36. Kurobane, Y., and Shiraishi, M., "Behavior of Yield Hinge at Girder End under Alternating Bending," Arch. Inst. of Japan, Fukuoka, Japan, Apr. 6, 1969.
37. Chipman, R. D., "Dimensionless Inelastic Bending Relationships," *Experimental Mechanics*, Feb. 1963.
38. Krawinkler, H., Bertero, V. V., and Popov, E. P., "Inelastic Behavior of Steel Beam-to-Column Subassemblages," Earthquake Engineering Research Center Report No. 71-7, University of California, Berkeley, Oct. 1971.
39. Driscoll, G. C., Jr., et al., "Plastic Design of Multi-Story Frames—Lecture Notes," Fritz Engineering Laboratory Report No. 273.20, Lehigh University, Aug. 1965.
40. Sheninger, E. L., and Lu, L. W., "Experiments on Non-Sway Structural Subassemblages," *Journal of the Structural Division, ASCE*, Vol. 96 (ST3), p. 573, March 1970.
41. Fielding, D. J., and Huang, J. S., "Shear in Steel Beam-to-Column Connections," *The Welding Journal*, Vol. 50, No. 7, p. 313-315, July 1971.
42. Fielding, D. J., Chen, W. F., and Beedle, L. S., "Frame Analysis and Connection Shear Deformation," Fritz Engineering Laboratory Report No. 333.16, January 1972.
43. Carpenter, L. D., "Behavior of Steel Frames Subjected to Gravity Load and Reversed Lateral Load," Ph.D. Dissertation, Lehigh University, 1972.
44. Kato, B., and Lu, L. W., "Instability Effects under Dynamic and Repeated Load," State-of-Art Report 3, Technical Committee 16, ASCE-IABSE International Conference on Tall Buildings, Aug. 1972.

## 8. Appendixes

### Appendix I Aseismic Forces of the Eight-Story Prototype Frame

#### DETERMINATION OF ASEISMIC DESIGN FORCES

The design forces were determined according to the procedure given in the Recommended Lateral Force Requirements of the Structural Engineers Association of California (SEAOC).

	Floor wt. $W_x$ , kips	Height $h_x$ , ft.	$W_x h_x$	Design Force $F_x$ , kips
 1	21.6	80	1728	1.38
2	21.6	70	1512	1.21
3	21.6	60	1296	1.04
4	21.6	50	1080	0.87
5	21.6	40	864	0.69
6	21.6	30	648	0.52
7	21.6	20	432	0.35
8	21.6	10	216	0.17
9	$\Sigma$ 172.8		7776	6.23

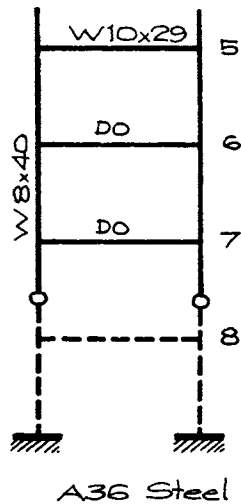
$$V = KCW \quad , \quad C = \frac{0.05}{T^{1/3}}$$

$$T = 0.8 \text{ sec.} \quad , \quad C = 0.0538$$

$$V = 0.67 \times 0.0538 \times 172.8 = 6.23 \text{ kips}$$

$$F_x = \frac{W_x h_x}{\Sigma W_x h_x} V \quad , \quad F_1 + F_2 + F_3 + F_4 + F_5 = 5.19 \text{ kips}$$

Member Sizes and Dimensions

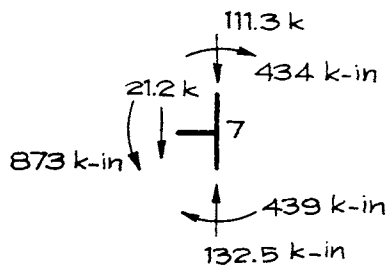


W 10x29  $I_x = 158 \text{ in}^4$  ,  $S_x = 30.8 \text{ in}^3$   
 c-to-c span = 15'-0"  
 clear span = 14'-3<sup>3</sup>/<sub>4</sub>"

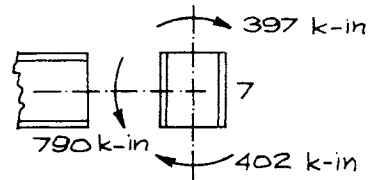
W 8x40  $I_x = 146 \text{ in}^4$  ,  $S_x = 35.5 \text{ in}^3$   
 $r_x = 3.53 \text{ in}$  ,  $r_y = 2.04 \text{ in}$   
 $A = 11.8 \text{ in}^2$   
 c-to-c height = 10'-0"  
 clear height = 9'-1<sup>3</sup>/<sub>4</sub>"

Bending Moments and Axial Loads

For the loading condition shown in Fig. 2.6 and with  $P = 17.28 \text{ kips}$  and  $H = 5.19 \text{ kips}$  , the following bending moments and axial loads were found to act at joint 7.



Acting on Centerlines



Acting on Clear Spans

Beam Check

$$f_b = \frac{790}{30.8} = 25.7 \text{ ksi} < 32 \text{ ksi} \quad \text{OK}$$

Allowable stress for combined gravity and seismic loads

Column Checks

The checks are made for the columns in the lowest story of the test frame. A full column height (not half height) is used.

$$G = \frac{\sum I_c/L_c}{\sum I_g/L_g} = 2.78 \quad \text{same for both ends}$$

Effective length factor  $K = 1.76$  (from alignment chart)

$$\frac{KL}{r_x} = \frac{1.76 \times 9.15 \times 12}{3.53} = 55, \quad \frac{L}{r_y} = \frac{9.15 \times 12}{2.04} = 54$$

$$F_a = 17.9 \text{ ksi}, \quad F_e' = 49.3 \text{ ksi}$$

Increased by  $1/3$  for combined gravity and seismic loads

$$F_a = 17.9 \times 4/3 = 23.9 \text{ ksi}, \quad F_e' = 49.3 \times 4/3 = 65.7 \text{ ksi}$$

$$F_b = 22 \times 4/3 = 29.4 \text{ ksi}$$

Bending and axial stresses

$$f_a = \frac{132.5}{11.8} = 11.2 \text{ ksi}, \quad f_b = \frac{402}{35.5} = 11.3 \text{ ksi}$$

Formula (1.6-1a)

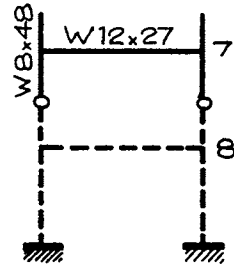
$$\frac{11.2}{23.9} + \frac{0.85 \times 11.3}{(1 - \frac{11.3}{65.7}) 29.4} = 0.469 + 0.394 = 0.863$$

Formula (1.6-1b)

$$\frac{11.2}{29.4} + \frac{11.3}{29.4} = 0.381 + 0.385 = 0.766$$



Member Sizes and Dimensions



A36 Steel

W12x27  $I_x = 204 \text{ in}^4$

c-to-c span = 15'-0"

clear span = 14'-3 1/2"

W8x48  $I_y = 60.9 \text{ in}^4$  ,  $S_y = 15.0 \text{ in}^3$

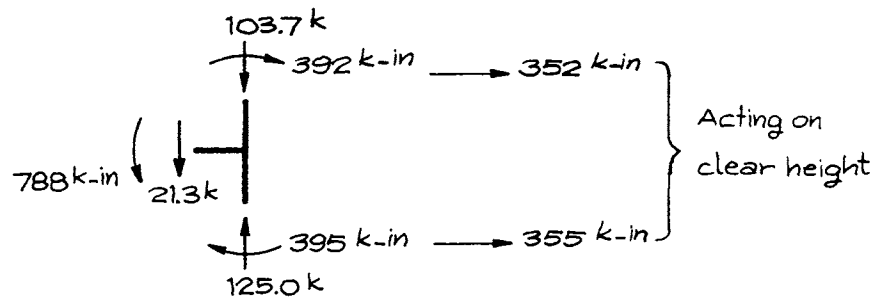
$A = 14.1 \text{ in}^2$  ,  $r_y = 2.08 \text{ in}$

c-to-c height = 10'-0"

clear height = 9'-0"

Bending Moments and Axial Loads

For the loading condition shown in Fig. 2.9 and with  $P = 17.28 \text{ kips}$  and  $H = 5.19 \text{ kips}$ , the following bending moments and axial loads were found to act at joint 7.



Column Checks

The checks are made for the lower columns of the test frame. A full column height (not half height) is used.

$$G = \frac{\sum I_c / L_c}{\sum I_g / L_g} = 0.9 \quad \text{same for both ends}$$

Effective length factor  $K=1.28$  (from alignment chart)

$$\frac{KL}{r_y} = \frac{1.28 \times 9 \times 12}{2.08} = 66$$

$$F_a = 16.9 \text{ ksi} \quad , \quad F_e' = 34.2 \text{ ksi}$$

Increased by  $1/3$  for combined gravity and seismic loads

$$F_a = 16.9 \times 4/3 = 22.5 \text{ ksi} \quad , \quad F_e' = 45.6 \text{ ksi}$$

$$F_b = 0.75 \times 36 \times 4/3 = 36 \text{ ksi} \quad , \quad 0.6 \times 36 \times 4/3 = 28.8 \text{ ksi}$$

Bending and axial stresses

$$f_a = \frac{125}{14.1} = 8.85 \quad , \quad f_b = \frac{355}{15.0} = 23.6$$

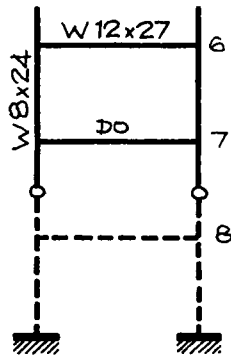
Formula (1.6-1a)

$$\frac{8.85}{22.5} + \frac{0.85 \times 23.6}{(1 - \frac{8.85}{45.6})36} = 0.393 + 0.692 = 1.085$$

Formula (1.6-1b)

$$\frac{8.85}{28.8} + \frac{23.6}{36} = 0.307 + 0.656 = 0.963$$

Member Sizes and Dimensions



A36 Steel

W12x27  $I_x = 204 \text{ in}^4$

c-to-c span = 15'-0"

clear span = 14'-4"

W8x24  $I_x = 82.5 \text{ in}^4$  ,  $S_x = 20.8 \text{ in}^3$

$r_x = 3.42 \text{ in}$  ,  $r_y = 1.61 \text{ in}$

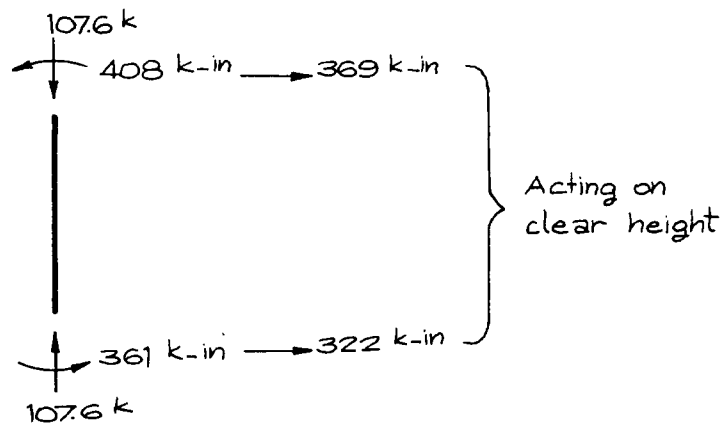
$A = 7.06 \text{ in}^2$

c-to-c height = 10'-0"

clear height = 9'-0"

Bending Moments and Axial Loads

Since the columns in the lowest story are reinforced by cover plates, the critical columns in the frame are those in the middle story (between joints 6 and 7). For the loading condition shown in Fig. 2.11 and with  $P = 17.28 \text{ kips}$  and  $H = 5.19 \text{ kips}$ , the bending moments and axial loads acting on the critical column are



Column Checks

$$G = \frac{\sum I_c/L_c}{\sum I_g/L_g} = 1.22 \quad \text{same for both ends}$$

Effective length factor  $K = 1.39$  (from alignment chart)

$$\frac{KL}{r_x} = \frac{1.39 \times 9 \times 12}{3.42} = 44 \quad , \quad \frac{L}{r_y} = \frac{9 \times 12}{1.61} = 67$$

$$F_a = 16.7 \text{ ksi} \quad , \quad F_e' = 77.1 \text{ ksi}$$

Increased by 1/3 for combined gravity and seismic loads

$$F_a = 16.7 \times 4/3 = 22.3 \text{ ksi} \quad , \quad F_e' = 77.1 \times 4/3 = 102.8 \text{ ksi}$$

$$F_b = 22 \times 4/3 = 29.4 \text{ ksi}$$

Bending and axial stresses

$$f_a = \frac{107.6}{7.06} = 15.3 \text{ ksi} \quad , \quad f_b = \frac{369}{20.8} = 17.7 \text{ ksi}$$

Formula (1.6-1a)

$$\frac{15.3}{22.3} + \frac{0.85 \times 17.7}{\left(1 - \frac{15.3}{102.8}\right) 29.4} = 0.699 + 0.602 = 1.301$$

Formula (1.6-1b)

$$\frac{15.3}{29.4} + \frac{17.7}{29.4} = 0.521 + 0.603 = 1.124$$

**Appendix 3 Cross-Sectional and Material Properties**

**TABLE AI. Average Section Properties\***

<i>Frame (1)</i>	<i>Section (2)</i>	<i>Flange width, <math>b_f</math> (in.) (3)</i>	<i>Flange Thickness, <math>t_f</math> (in.) (4)</i>	<i>Depth, <math>d</math> (in.) (5)</i>	<i>Web thickness, <math>t_w</math> (in.) (6)</i>	<i>Area, <math>A</math> (in.<sup>2</sup>) (7)</i>	<i>Moment of inertia about x-x axis, <math>I_x</math> (in.<sup>4</sup>) (8)</i>	<i>Moment of inertia about y-y axis, <math>I_y</math> (in.<sup>4</sup>) (9)</i>
Frame A	W10×29	5.800 (5.799)	0.520 (0.500)	10.37 (10.22)	0.304 (0.289)	8.87 (8.54)	167 (158)	16.9 (16.3)
	W8×40	8.075 (8.077)	0.543 (0.558)	8.24 (8.25)	0.376 (0.365)	11.5 (11.8)	141 (146)	47.6 (49.0)
Frame B	W10×29	5.786	0.523	10.37	0.310	8.94	168	16.9
	W8×40	8.036	0.556	8.28	0.384	11.7	145	48.1
Frame C	Welded beam	7.899	0.390	10.42	0.321	9.25	179	32.1
	W8×40	8.075	0.543	8.24	0.376	11.5	141	47.7
Frame D	W12×27	6.514 (6.497)	0.393 (0.400)	12.02 (11.94)	0.264 (0.237)	8.09 (7.95)	204 (204)	18.1 (18.3)
	W8×48	8.158 (8.117)	0.677 (0.683)	8.50 (8.50)	0.439 (0.405)	14.1 (14.1)	182 (184)	61.3 (60.9)
Frame E	W12×27	6.514	0.393	12.03	0.264	8.09	204	18.1
	W8×24	6.521 (6.500)	0.404 (0.398)	7.95 (7.93)	0.248 (0.245)	7.04 (7.06)	82 (83)	18.7 (18.2)

\* The values in parentheses are handbook values.

**TABLE AII. Static Yield Stresses, Plastic Moments and Axial Yield Loads\***

<i>Frame (1)</i>	<i>Section (2)</i>	<i>Avg. static yield stress, <math>\sigma_y</math> (ksi)</i>		<i>Axial yield load, <math>P_y</math> (ksi) (5)</i>	<i>Plastic moment about x-x axis, <math>M_{px}</math> (kip-in.) (6)</i>	<i>Plastic moment about y-y axis, <math>M_{py}</math> (kip-in.) (7)</i>
		<i>Flange (3)</i>	<i>Web (4)</i>			
Frame A	W10×29	34.65 (36.0)	41.10 (36.0)	325 (304)	1301 (1235)	311 (309)
	W8×40	35.20 (36.0)	35.70 (36.0)	404 (418)	1360 (1415)	632 (663)
Frame B	W10×29	34.73	41.60	330	1315	313
	W8×40	37.65	42.50	453	1507	687
Frame C	Welded beam	34.61	37.66	329	1349	430
	W8×40	35.20	35.70	404	1360	632
Frame D	W12×27	34.98 (36.0)	41.79 (36.0)	303 (283)	1389 (1351)	299 (309)
	W8×48	30.11 (36.0)	32.94 (36.0)	435 (503)	1485 (1745)	689 (820)
Frame E	W12×27	35.06	42.03	304	1394	300
	W8×24	35.42 (36.0)	36.84 (36.0)	251 (249)	820 (813)	308 (306)

\* The values in parentheses are based on handbook properties and an assumed yield stress of 36 ksi.

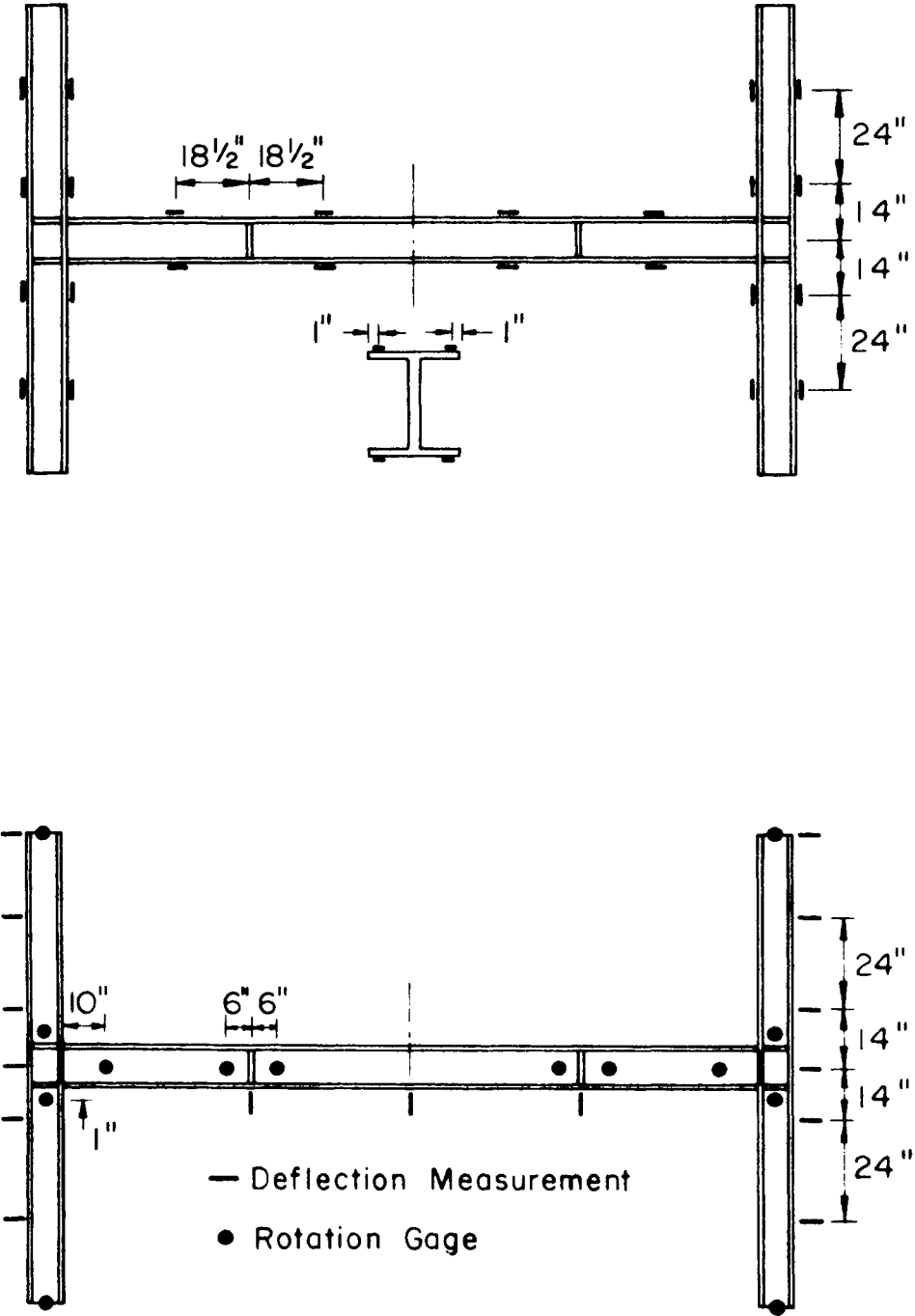


FIGURE A1. Instrumentation for Frame A

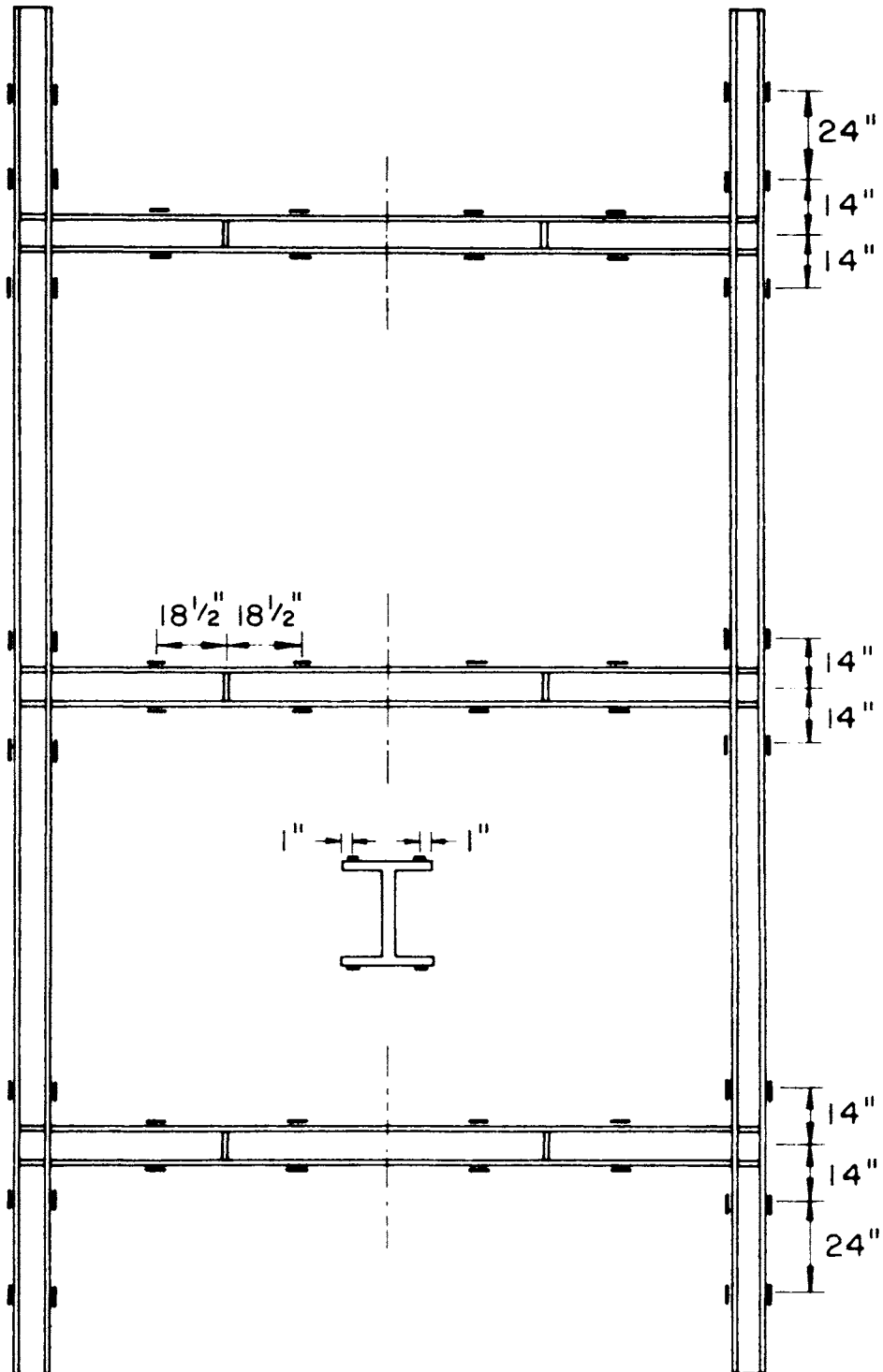


FIGURE A2. Instrumentation for Frame B (strain gage locations)

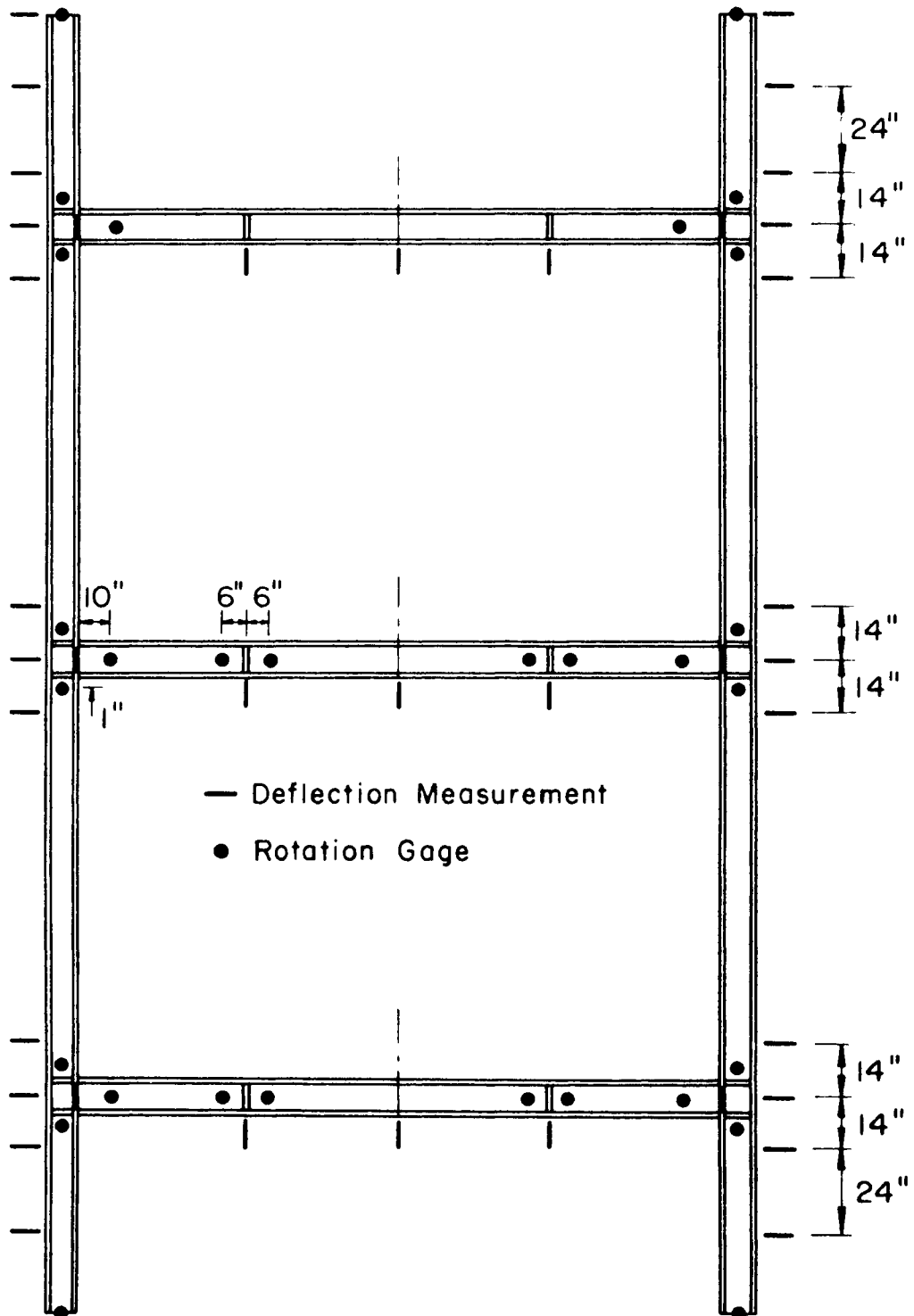


FIGURE A3. Instrumentation for Frame B (locations for deflection and rotation measurements)



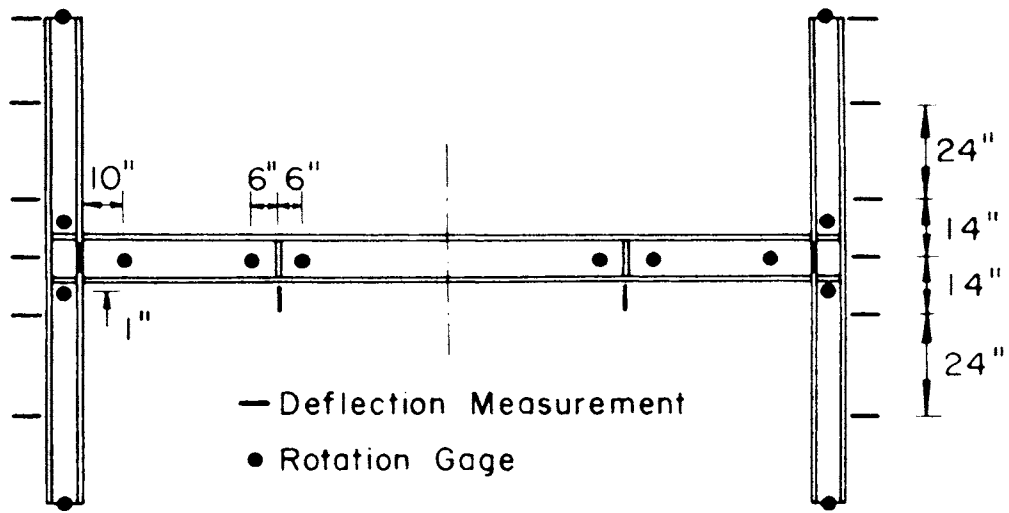
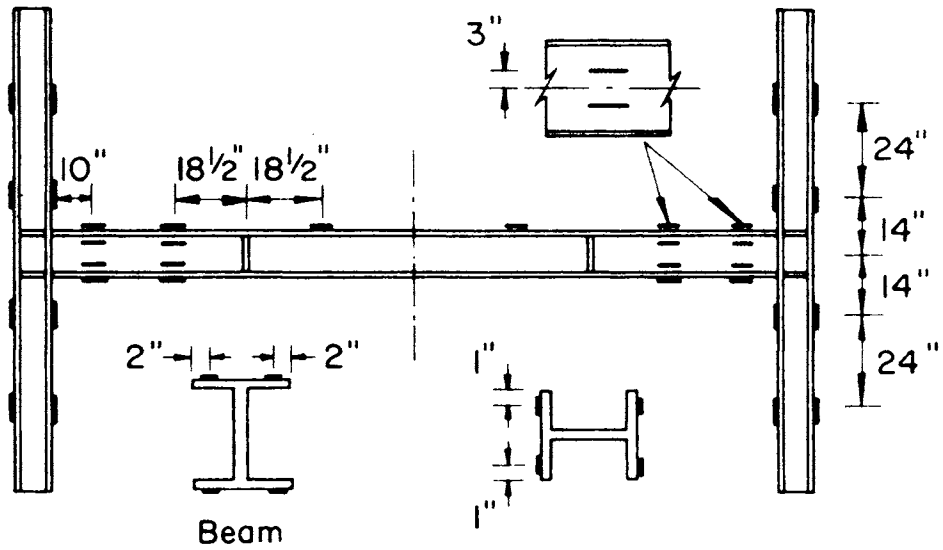


FIGURE A4. Instrumentation for Frame C

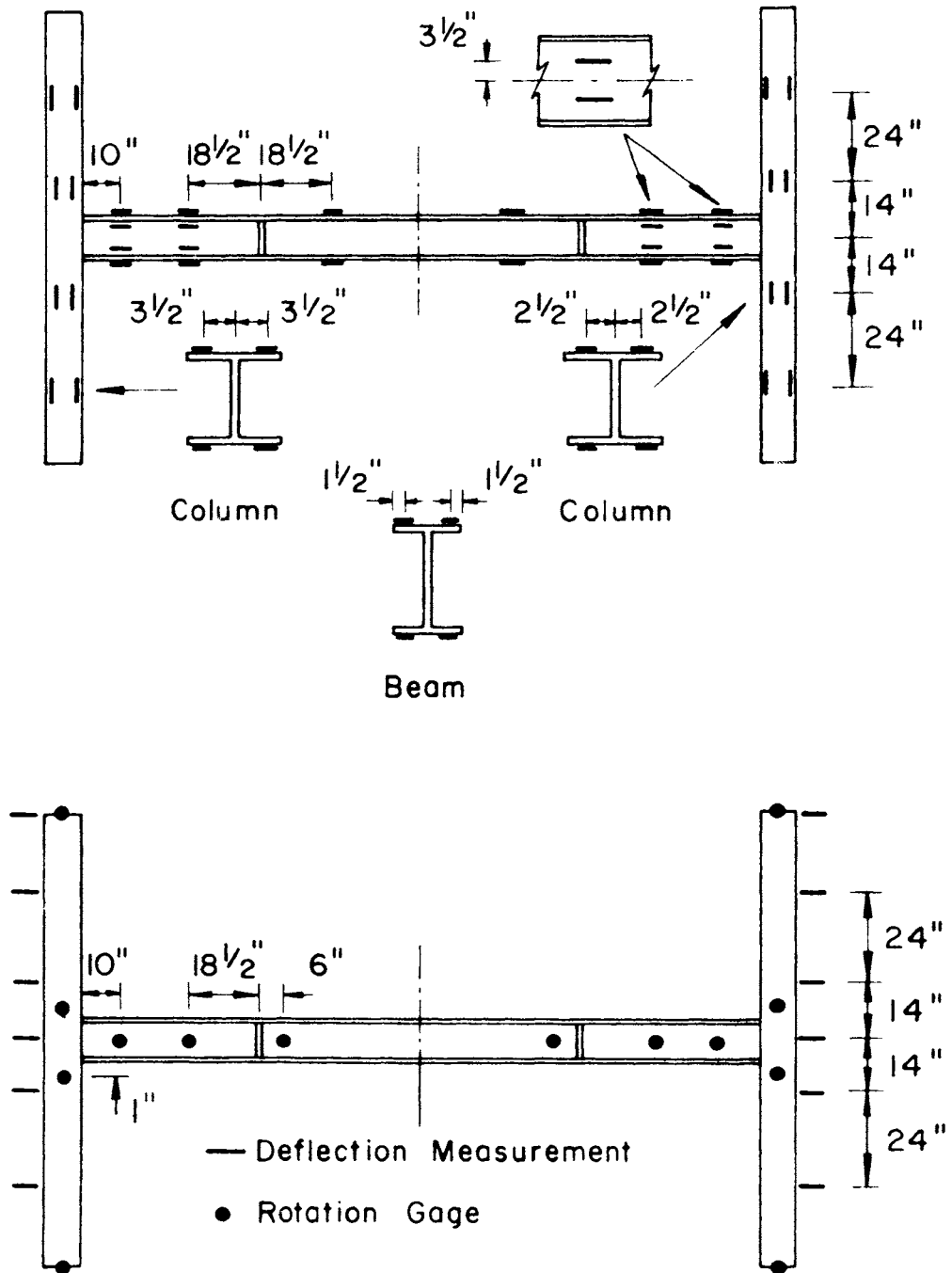


FIGURE A5. Instrumentation for Frame D

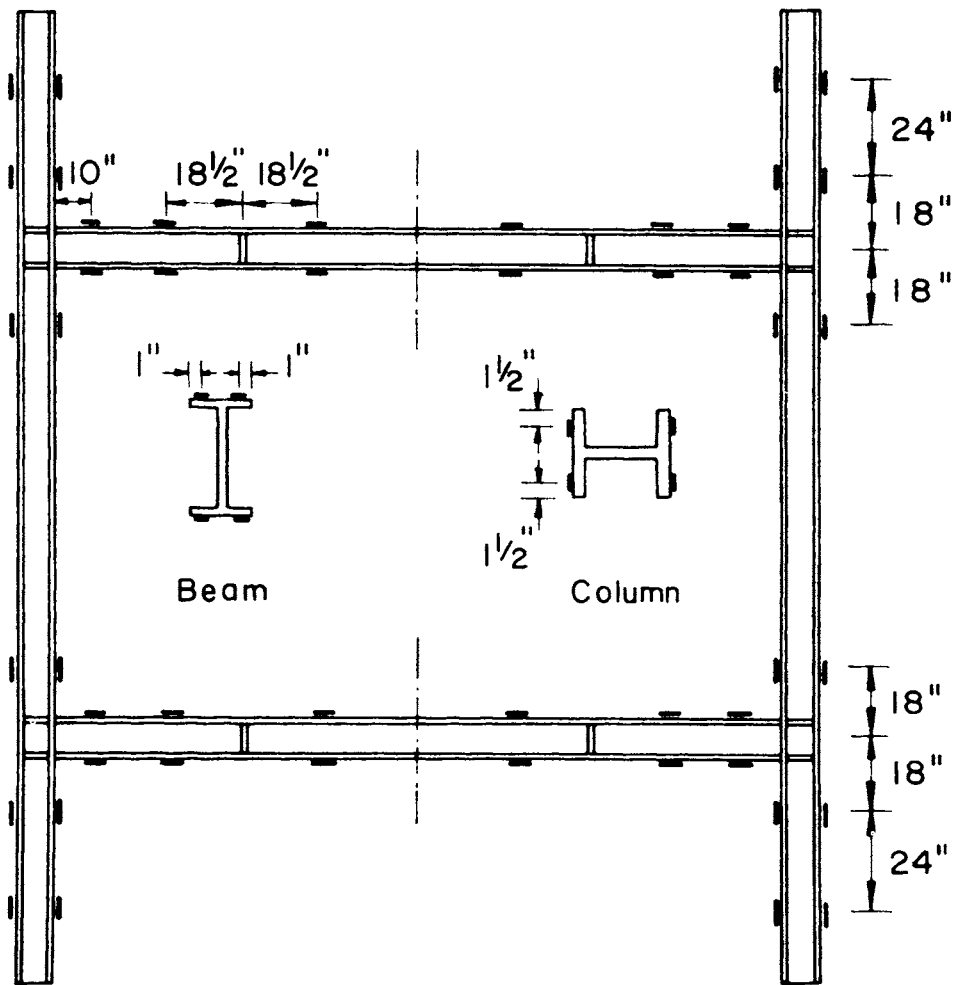


FIGURE A6. Instrumentation for Frame E (strain gage locations)

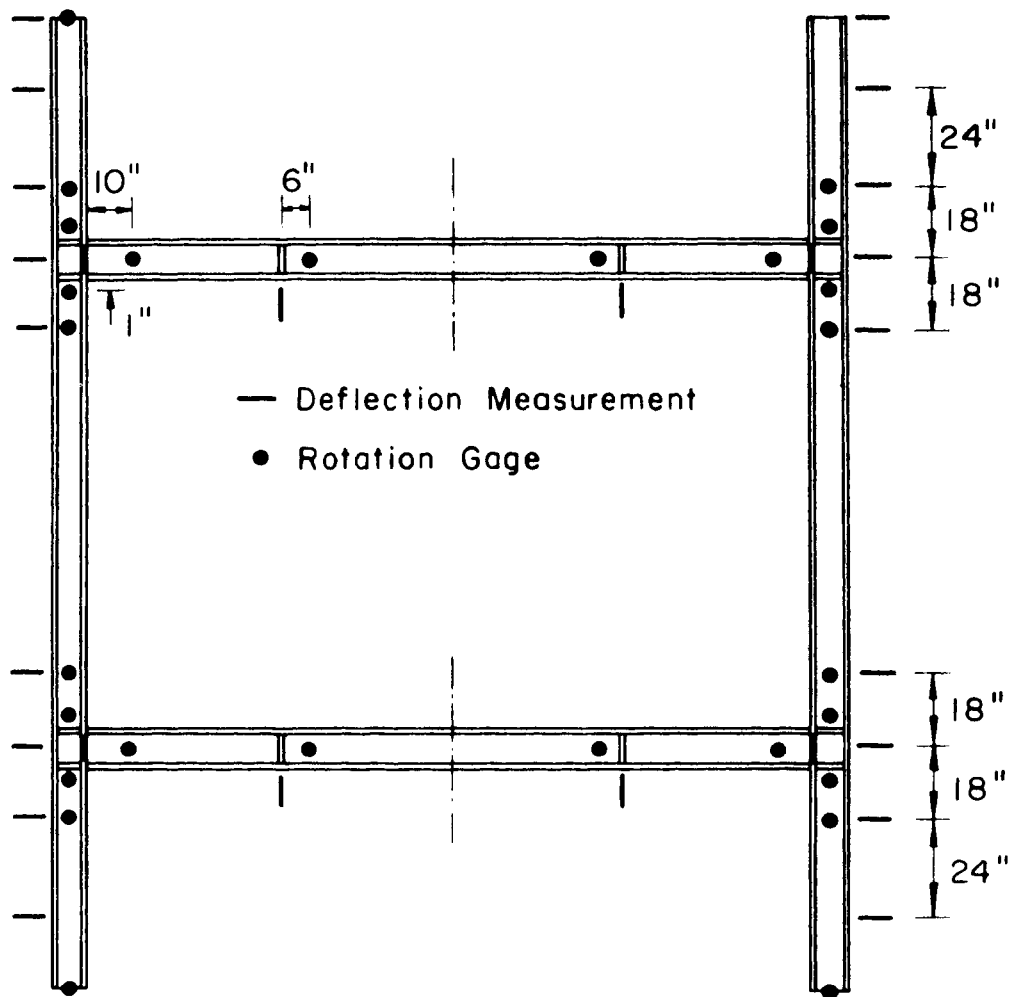


FIGURE A7. Instrumentation for Frame E (locations for deflection and rotation measurements)

# BULLETINS

## Steel Research for Construction

- No. 1 Current Paving Practices on Orthotropic Bridge Decks—*Battelle Memorial Institute, October, 1965*
- No. 2 Strength of Three New Types of Composite Beams—*A. A. Toprac, October, 1965*
- No. 3 Research on and Paving Practices for Wearing Surfaces on Orthotropic Steel Bridge Decks, Supplement to Bulletin 1—*Battelle Memorial Institute, August, 1966*
- No. 4 Protection of Steel Storage Tanks and Pipe Underground—*Battelle Memorial Institute, May, 1967*
- No. 5 Fatigue Strength of Shear Connectors—*R. G. Slutter and J. W. Fisher, October, 1967*
- No. 6 Paving Practices for Wearing Surfaces on Orthotropic Steel Bridge Decks, Supplement to Bulletins 1 and 3—*Battelle Memorial Institute, January, 1968*
- No. 7 Report on Investigation of Orthotropic Plate Bridges—*D. Allan Firmage, February, 1968*
- No. 8 Deformation and Energy Absorption Capacity of Steel Structures in the Inelastic Range—*T. V. Galambos, March, 1968*
- No. 9 The Dynamic Behavior of Steel Frame and Truss Buildings—*Dixon Rea, J. G. Bouwkamp and R. W. Clough, April, 1968*
- No. 10 Structural Behavior of Small-Scale Steel Models—*Massachusetts Institute of Technology, April, 1968*
- No. 11 Response of Steel Frames to Earthquake Forces—Single Degree of Freedom Systems—*M. J. Kaldjian and W. R. S. Fan, November, 1968*
- No. 12 Response of Multistory Steel Frames to Earthquake Forces—*Subhash C. Goel, November, 1968*
- No. 13 Behavior of Steel Building Connections Subjected to Inelastic Strain Reversals—*E. P. Popov and R. B. Pinkney, November, 1968*
- No. 14 Behavior of Steel Building Connections Subjected to Inelastic Strain Reversals—Experimental Data—*E. P. Popov and R. B. Pinkney, November, 1968*
- No. 15 Tentative Criteria for Load Factor Design of Steel Highway Bridges—*George S. Vincent, March, 1969*
- No. 16 Strength of Plate Girders with Longitudinal Stiffeners—*Lehigh University, April, 1969*
- No. 17 Fatigue Strength of Plate Girders—*Lehigh University, April, 1969*
- No. 18 Interior Corrosion of Structural Steel Closed Sections—*February, 1970*
- No. 19 Criteria for the Deflection of Steel Bridges—*R. N. Wright and W. H. Walker, November, 1971*
- No. 20 Addendum Report on Paving Practices for Wearing Surfaces on Orthotropic Steel Bridge Decks—*Battelle Memorial Institute, October, 1971*
- No. 21 Cyclic Loading of Full-Size Steel Connections—*E. P. Popov and R. M. Stephen, February, 1972*
- No. 22 Seismic Behavior of Multistory Braced Steel Frames—*S. C. Goel and R. D. Hanson, April, 1972*
- No. 23 Plastic Subassemblage Analysis and Tests for Rigid High-Rise Steel Frames—*Lehigh University, March, 1973*
- No. 24 Reversed and Repeated Load Tests of Full-Scale Steel Frames—*L. D. Carpenter and L. W. Lu, April, 1973*

Committee of Structural Steel Producers

•

Committee of Steel Plate Producers

**american iron and steel institute**

150 East 42nd Street, New York, N.Y. 10017

